Supporting Information

Bioorthogonal Probes for L-Form Conversion Visualization and Insights into Antimicrobial Resistance

Yunzhe Tao [a], Yongwei Feng [ba], Yu Peng [a], Xiang Wang [a], Xiangchuan Meng [a], Youjun Xu [b], Xiaowan Han *[a], Qingyang Zhang *[a], Hai-Yu Hu *[a]

[a]State Key Laboratory of Bioactive Substance and Function of Natural Medicines, Institute of Materia Medica, Chinese Academy of Medical Sciences and Peking Union Medical College, Beijing, 100050, China.

[b]School of Pharmaceutical Engineering and Key Laboratory of Structure-Based Drug Design & Discovery (Ministry of Education), Shenyang Pharmaceutical University, Shenyang, 110016, China.

Table of Contents

Abbreviations

ATCC = American Type Culture Collection
B. subtilis = *Bacillus subtilis*
CWDB = cell wall-deficient bacteria
D-Ala = D-Alanine
DCM = Dichloromethane
DEA = Diethylamine
DFT = density functional theory
DIPEA = N,N-Diisopropylethylamine
DMSO = Dimethyl Sulfoxide
DMF = N,N-Dimethylformamide
E. coli = *Escherichia coli*
ESI = Electrospray Ionization
ETDS = Energy Transfer to a Dark State
HPLC = High Performance Liquid Chromatography
HRMS = High-resolution Mass Spectrometry
LB = Lysogeny broth
LC-MS = Liquid chromatography-mass spectrometry
MeOH = Methanol
MSM = magnesium-sucrose-maleic acid
NMR = Nuclear Magnetic Resonance
OD = Optical Density
PBS = Phosphate-Buffered Saline
PE = petroleum ether
rt = Room Temperature
S. aureus = *Staphylococcus aureus*
SD = Standard Deviation
TD-DFT = time-dependent density functional theory
TSB = Tryptic Soy Broth
TMP = Trimethoprim

1. Experimental Procedures

1.1 General methods

All chemicals were purchased from Innochem and Bidepharm. Commercially available reagents were used without further purification. Lysostaphin(Lysostaphin from *Staphylococcus staphylolyticus*, CAS: 9011-93-2) was purchased from Sigma-Aldrich (shanghai) Trading Co., Ltd. The bacterial strain *Staphylococcus aureus (S. aureus*, ATCC 29213, ATCC 33592, RN 4220), *Bacillus subtilis (B. subtilis*, ATCC 6633), *Escherichia coli (E. coli*, ATCC 25922) were purchased from the American Type Culture Collection (ATCC), USA. The UV-vis absorption and fluorescence emission spectra were read in a Tecan Spark™ 10M Multimode Microplate Reader. ^{1}H NMR and ^{13}C NMR spectra were recorded at 400 MHz or 500 MHz and 101 MHz or 125 MHz, respectively. HRMS was measured using a Thermo LCQ Deca XP Max mass spectrometer for ESI. Confocal fluorescence images were captured on an ISS Q2 confocal laser scanning system coupled with a Nikon TE2000 microscope with a 60×/1.2 NA WI objective lens. NB/MSM or NA/MSM medium is composed of 2×magnesium-sucrose-maleic acid (MSM) pH 7 (40 mM $MgCl_2$, 1 M sucrose, and 40 mM maleic acid) mixed 1:1 with 2× NB or 2× NA. For bacteria induced in Liquid conditions, 1~2 μl cells were sampled and mounted on microscope slides covered with a thin film of 1% agarose in water, or in MSM for L-form. For bacteria induced by solid agar, 1~2 μl cells were firstly placed on 35 mm sterile glass bottom microwell dishes and then a thin layer of antibiotic-contained NB/MSM with 1% agar was placed on the top of the dishes. Images were acquired with ISS VistaVision and processed by ImageJ.

1.2 Synthetic procedures and characterized data

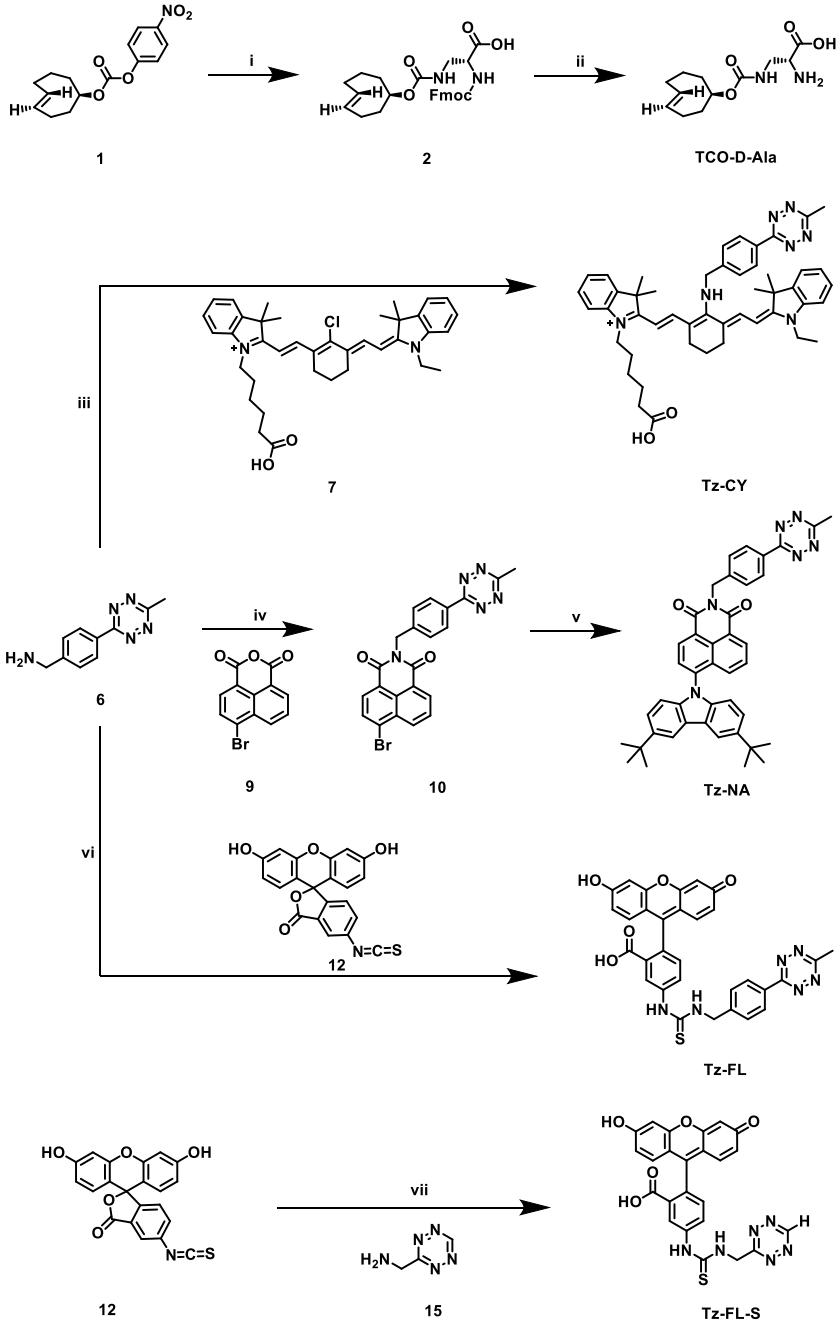

Scheme S1. Synthesis of **TCO-D-Ala**, **Tz-CY**, **Tz-NA**, **Tz-FL**, and **Tz-FL-S**. Reaction conditions: (i) Fmoc-2,3-diaminopropionic acid, DIPEA, DMF, rt, 12 h; (ii) DEA, DCM, rt, 1.5 h; (iii) DIPEA, DMF, rt, under argon, 48 h; (iv) EtOH, 90°C, 2h; (v) 3,6-di-tert-butyl-9H-carbazole, $Pd_2(DBA)_3$, RuPhos, t-BuOK, Toluene, 115°C, under argon, 1.5 h; (vi) DIPEA, DMF, rt, under argon, 3 h; (vii) DIPEA, DMF, rt, under argon, 1 h.

(R)-2-((((9H-fluoren-9-yl)methoxy)carbonyl)amino)-3-(((((R,E)-cyclooct-4-en-1-yl)oxy)carbonyl)amino)propanoic acid (2)

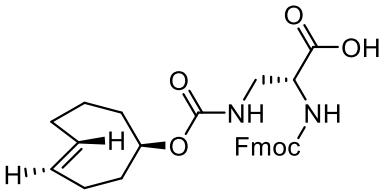

Fmoc-2,3-diaminopropionic acid (171 mg, 0.52 mmol) was dissolved in 5 mL dry DMF. Next, (R,E)-cyclooct-4-en-1-yl (4-nitrophenyl) carbonate (compound **1**, 149 mg, 0.51 mmol) was added. Finally, DIPEA (0.926 mL, 5.5 mmol) was added. The yellow solution was stirred at rt for 12 h until carbonate was consumed monitored by TLC. The solution was concentrated and the remaining brown oil was purified by flash chromatography eluting with DCM/MeOH = 20:1 to 10:1 to obtain the product as a white foamy solid (177 mg, 72%). TLC (DCM/MeOH 16:1): R_f = 0.25. ^{1}H NMR (400 MHz, DMSO-d_6) δ 12.71 (s, 1H), 7.89 (d, *J* = 7.5 Hz, 2H), 7.71 (d, *J* = 7.4 Hz, 2H), 7.50 (d, *J* = 8.2 Hz, 1H), 7.42 (t, *J* = 7.5 Hz, 2H), 7.33 (t, *J* = 7.4 Hz, 2H), 7.00 (s, 1H), 5.61 – 5.50 (m, 1H), 5.46 – 5.34 (m, 1H), 4.32 – 4.14 (m, 4H), 4.14 – 4.02 (m, 1H), 3.33 – 3.20 (m, 2H), 2.30 – 2.11 (m, 3H), 1.95 – 1.77 (m, 4H), 1.68 – 1.42 (m, 3H). HRMS (m/z) [M+H]+: Calcd. for $C_{27}H_{31}O_6N_2$+ 479.2177, found 479.2187.

(R)-2-amino-3-(((((R,E)-cyclooct-4-en-1-yl)oxy)carbonyl)amino)propanoic acid (TCO-D-Ala)

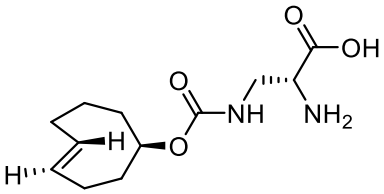

Compond **2** (64 mg, 0.13 mmol) was dissolved in 1 mL DCM. Then 1 mL of DEA was added. The mixture was stirred at rt for 2 h. After the starting material was consumed, the solvent was removed under vacuum. The residue was suspended in 2 mL water and filtered using a syringe combined with a nylon filtration membrane. Then, further purification for biological studies was conducted by injecting the filtrate into HPLC and the product was obtained by lyophilization as a white powder (29 mg, 84%) . (Method used: solvent A: H_2O + 0.1% HCOOH; solvent B: CH_3CN; gradient: 5% B → 50% B in 15 min, then 95% B for 10 min and 5% B for 5 min). The product eluates at 13 min (on a Shiseido® C18 column (5 µm, 250 × 10 mm) at 4.7 mL/min flow rate). ^{1}H NMR (400 MHz, Deuterium Oxide) δ 5.79 – 5.63 (m, 1H), 5.63 – 5.49 (m, 1H), 4.32 (s, 1H), 3.86 (s, 1H), 3.74 – 3.63 (m, 1H), 3.58 – 3.45 (m, 1H), 2.43 – 2.26 (m, 3H), 2.21 – 1.84 (m, 4H), 1.82 – 1.56 (m, 3H). ^{13}C NMR (101 MHz, Deuterium Oxide) δ 172.07, 158.66, 135.64, 133.39, 82.40, 55.12, 40.92, 40.30, 37.72, 33.68, 32.00, 30.55. HRMS (m/z) [M+H]+: Calcd. for $C_{12}H_{21}O_4N_2$+ 257.1496, found 257.1507.

tert-butyl (4-cyanobenzyl)carbamate (4)

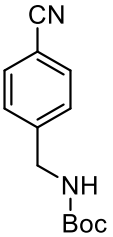

To a solution of 4-(aminoethyl)benzonitrile (2.00 g, 15.1 mmol) in DCM (4 mL) was added Boc_2O (3.63 g, 16.6 mmol), and the mixture was left stirring at rt for 16 h. After the reaction, the solvent was removed under vacuum and the residue was slurred with methanol, filtered, and the filter cake was rinsed with a small amount of methanol and dried to obtain the product as a white solid (2.88 g, 82%). TLC (PE/EtOAc 3:1): R_f = 0.5. ^{1}H NMR (400 MHz, Chloroform-*d*) δ 7.62 (d, *J* = 7.9 Hz, 2H), 7.38 (d, *J* = 7.9 Hz, 2H), 4.96 (s, 1H), 4.37 (d, *J* = 5.9 Hz, 2H), 1.46 (s, 9H). HRMS-ESI (m/z): [M+H]+ calcd for $C_{13}H_{17}N_2O_2$+ 233.1285, found 233.1284.

tert-butyl (4-(6-methyl-1,2,4,5-tetrazin-3-yl)benzyl)carbamate (5)

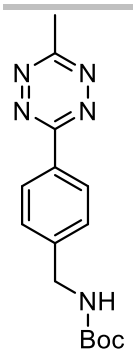

To a 50 mL schlenk tube equipped with a stir bar, compound **4** (2.0 g, 8.61 mmol), 3-Mercaptopropionic acid (457 mg, 4.30 mmol), hydrazine hydrate (4.18 ml, 86.1 mmol) and Acetonitrile (4.5 mL, 86.1 mmol) was added. The tube was sealed and heated in an oil bath at 60°C for 24 hours. After reaction, the mixture was cooled to room temperature and transferred into an Erlenmeyer flask. Sodium nitrite (11.88 g, 172.2 mmol) in 40 mL of water was added and followed by slow addition of 1M HCl at 0℃ until the pH value ≈ 3. (Caution! Toxic nitrogen oxide gasses generated.) The mixture was extracted with CH_2Cl_2 (4×50 mL) and the organic phase was dried over anhydrous sodium sulfate and filterd. The solvent was removed using rotary evaporation and the residue was further purified by silica column chromatography eluting with Et_2O/DCM(1:20). The product was obtained as a purple solid (1.03 g, 40%). TLC (Et_2O/DCM 1:10): R_f = 0.5. ^{1}H NMR (400 MHz, Chloroform-*d*) δ 8.55 (d, *J* = 7.9 Hz, 2H), 7.50 (d, *J* = 7.9 Hz, 2H), 4.98 (s, 1H), 4.44 (s, 2H), 3.09 (s, 3H), 1.48 (s, 9H). HRMS-ESI (m/z): [M+H]+ calcd for $C_{15}H_{20}N_5O_2$+ 302.1612, found 302.1615.

(4-(6-methyl-1,2,4,5-tetrazin-3-yl)phenyl)methanamine (6)

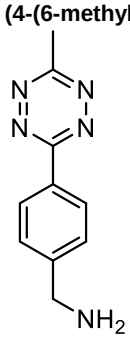

In a 100 mL round-bottom flask, compound **5** (450mg, 1.5mmol) was dissolved in DCM (4 mL) and Trifluoroacetic acid (3 mL) was added, and the mixture was left stirring at rt for 0.5 h. The volatiles were removed under reduced pressure and the remaining residue was dissolved in 30 mL EtOAc and washed with sat. aq $NaHCO_3$ (30 mL) in a separatory funnel. The two phases were separated, and the aqueous layer was further extracted with EtOAc (2 × 30 mL). The combined organic layers were pooled together and dried over anhydrous Na_2SO_4, and the solvent was removed in vacuo. The pink solid was collected and dried under vacuum to yield compound **6** (236 mg, 79%). The crude material was considered pure enough for subsequent reactions and the identity was confirmed by HRMS-ESI (m/z): [M+H]+ calcd for $C_{10}H_{12}N_5$+ 202.1088, found 202.1089.The crude was used directly without further purification.

2-((E)-2-((E)-3-(2-((E)-1-(5-carboxypentyl)-3,3-dimethylindolin-2-ylidene)ethylidene)-2-((4-(6-methyl-1,2,4,5-tetrazin-3-yl)benzyl)amino)cyclohex-1-en-1-yl)vinyl)-1-ethyl-3,3-dimethyl-3H-indol-1-ium (Tz-CY)

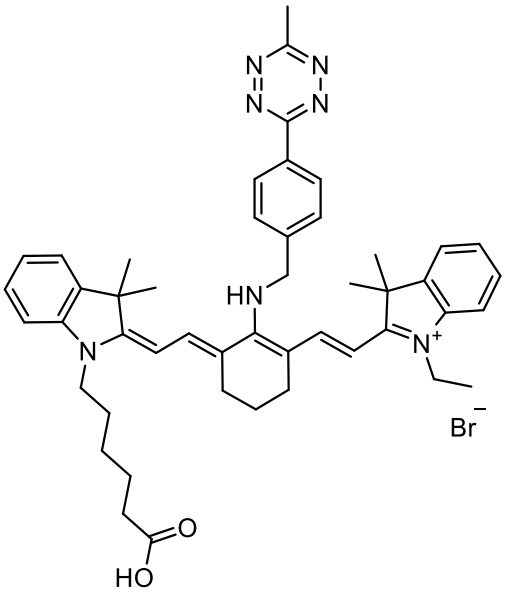

Compound **7** (55 mg, 0.08 mmol),[1] compound **6** (68 mg, 0.34 mmol), DIPEA (28 μL, 0.16 mmol) was dissolved in 4 mL dry DMF under an argon atmosphere. The mixture was stirred at 40℃ for 48 h . The solvent was removed under vacuum and the residue was purified by silica column chromatography eluting with MeOH:DCM (19:1 to 8:1). The product was obtained as a dark blue solid (59 mg, 86%). ^{1}H NMR (500 MHz, Chloroform-*d*) δ 8.57 (d, *J* = 8.0 Hz, 2H), 7.75 – 7.64 (m, 4H), 7.25 – 7.21 (m, 2H), 7.17 (t, *J* = 7.3 Hz, 2H), 7.02 (q, *J* = 7.3 Hz, 2H), 6.84 (t, *J* = 8.4 Hz, 2H), 5.63 (dd, *J* = 13.2, 6.7 Hz, 2H), 5.15 (s, 2H), 3.85 (d, *J* = 39.8 Hz, 4H), 3.09 (s, 3H), 2.49 (q, *J* = 6.3 Hz, 4H), 2.39 (t, *J* = 7.2 Hz, 2H), 1.86 – 1.80 (m, 2H), 1.80 – 1.74 (m, 2H), 1.72 – 1.67 (m, 2H), 1.52 – 1.43 (m, 14H), 1.32 (t, *J* = 7.2 Hz, 3H).^{13}C NMR (126 MHz, Chloroform-*d*) δ 177.46, 167.43, 143.44, 139.16, 138.95, 131.28, 129.00, 128.68, 128.21, 123.02, 122.97, 122.20, 121.36, 121.02, 108.60, 108.44, 94.69, 76.91, 52.57, 47.96, 33.96, 28.80, 28.71, 26.49, 26.44, 25.50, 24.52, 21.62, 21.30, 11.65. HRMS-ESI (m/z) [M]+: Calcd. for $C_{48}H_{56}O_2N_7$+ 762.4490, found 762.4493.

6-bromo-2-(4-(6-methyl-1,2,4,5-tetrazin-3-yl)benzyl)-1H-benzo[de]isoquinoline-1,3(2H)-dione (10)

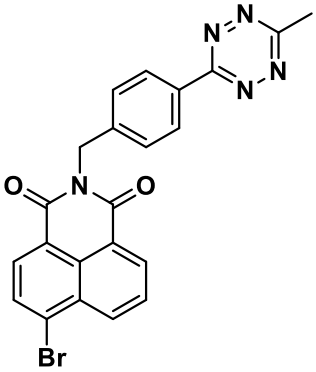

The compound **6** (50 mg, 0.25 mmol) was taken into a 25 mL round-bottom flask, 6-bromo-1H,3H-benzo[de]isochromene-1,3-dione(compound **9**, 35 mg, 0.13 mmol) and EtOH (2mL) was added. The mixture was stirred at 90℃ for 2 h. After the reaction, the mixture was filtered and the filter cake was rinsed with little methanol and dried. The product was obtained as a red solid (53 mg, 91%). ^{1}H NMR (400 MHz, Chloroform-*d*) δ 8.70 (d, *J* = 7.3 Hz, 1H), 8.60 (d, *J* = 8.6 Hz, 1H), 8.54 (d, *J* = 8.0 Hz, 2H), 8.45 (d, *J* = 7.9 Hz, 1H), 8.06 (d, *J* = 7.9 Hz, 1H), 7.87 (t, *J* = 8.1 Hz, 1H), 7.72 (d, *J* = 8.0 Hz, 2H), 5.47 (s, 2H), 3.07 (s, 3H). HRMS-ESI (m/z): [M+H]+ calcd for $C_{22}H_{15}BrN_5O_2$+ 460.0404, found 460.0411.

6-(3,6-di-tert-butyl-9H-carbazol-9-yl)-2-(4-(6-methyl-1,2,4,5-tetrazin-3-yl)benzyl)-1H-benzo[de]isoquinoline-1,3(2H)-dione (Tz-NA)

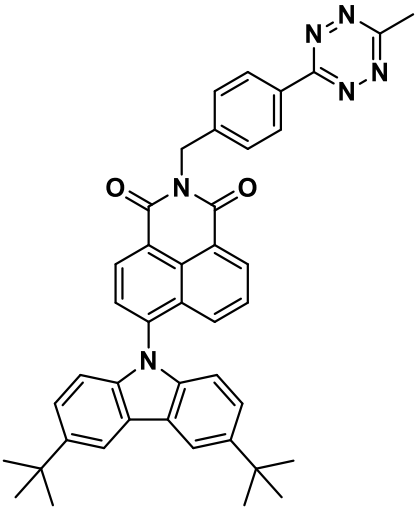

To a 50 mL flame-dried round-bottom flask and under an argon atmosphere, compond **10** (23 mg, 0.05 mmol) was dissolved in 2 mL toluene, and 3,6-di-tert-butyl-9H-carbazole(16 mg, 0.057 mmol), Potassium tert-butoxide(11 mg, 0.01 mmol), RuPhos(14 mg, 0.03 mmol), $Pd_2(DBA)_3$(7 mg, 0.0076 mmol) was added. The mixture was stirred at 110℃ for 10 h. The solvent was removed in vacuo and the residue was purified by silica column chromatography eluting with PE: EtOAc (6:1) and further purified by PTLC using an elution of PE/MeOH/ EtOAc (5:1:1). The product was obtained as a dark red solid(11 mg, 33%).^{1}H NMR (400 MHz, Chloroform-*d*) δ 8.81 (d, *J* = 7.8 Hz, 1H), 8.71 (dd, *J* = 7.3, 1.2 Hz, 1H), 8.61 – 8.54 (m, 2H), 8.20 (d, *J* = 1.9 Hz, 2H), 7.95 (dd, *J* = 8.5, 1.2 Hz, 1H), 7.89 (d, *J* = 7.8 Hz, 1H), 7.83 – 7.76 (m, 2H), 7.66 (dd, *J* = 8.5, 7.3 Hz, 1H), 7.41 (dd, *J* = 8.6, 1.9 Hz, 2H), 6.96 (d, *J* = 8.6 Hz, 2H), 5.55 (s, 2H), 3.08 (s, 3H), 1.47 (s, 18H).^{13}C NMR (101 MHz, Chloroform-*d*) δ 167.22, 164.11, 163.94, 163.71, 143.87, 141.98, 141.43, 140.19, 132.38, 132.06, 131.01, 130.91, 129.85, 129.68, 129.03, 128.18, 127.50, 126.99, 124.06, 123.95, 123.19, 122.01, 116.57, 109.50, 43.53, 34.84, 32.00, 21.18. HRMS-ESI (m/z) [M+H]+: Calcd. for $C_{42}H_{39}O_2N_6$+ 659.3129, found 659.3152.

2-(6-hydroxy-3-oxo-3H-xanthen-9-yl)-5-(3-(4-(6-methyl-1,2,4,5-tetrazin-3-yl)benzyl)thioureido)benzoic acid (Tz-FL)

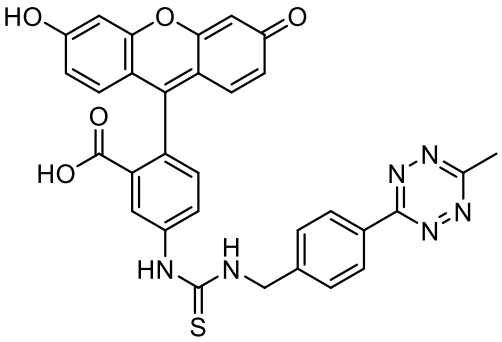

To a solution of compound **6** (16 mg, 0.08 mmol) in anhydrous DMF (2 mL) was added DIPEA (34 µL, 0.2 mmol) followed by fluorescein-5-isothiocyanate (compound **12**, 31 mg, 0.08 mmol) under an argon atmosphere. The reaction mixture was stirred in the dark at room temperature for 3 h and then concentrated in vacuo. The crude product was purified by preparation thin layer chromatography with DCM : MeOH = 10 : 1. The product was obtained as a red orange solid (41 mg, 87%).[2] For further purification, methanol was used to dissolve the product and injected into HPLC. (Method used: solvent A: H_2O + 0.1% HCOOH; solvent B: CH_3CN; gradient: 5% B → 80% B in 25 min, then 95% B for 5 min and 5% B for 5 min). The product eluates at 22 min (on a Shiseido® C18 column (5 µm, 250 × 10 mm) at 4.7 mL/min flow rate). ^{1}H NMR (400 MHz, Methanol-d_4) δ 8.51 (d, *J* = 6.3 Hz, 2H), 8.16 (s, 1H), 7.80 (d, *J* = 8.3 Hz, 1H), 7.63 (d, *J* = 7.1 Hz, 2H), 7.16 (d, *J* = 6.2 Hz, 1H), 6.66 (d, *J* = 6.6 Hz, 4H), 6.52 (d, *J* = 8.7 Hz, 2H), 4.99 (s, 2H), 3.02 (s, 3H). HRMS-ESI (m/z) [M+H]+: Calcd. for $C_{31}H_{23}O_5N_6S$+ 591.1446, found 591.1437.

tert-butyl ((1,2,4,5-tetrazin-3-yl)methyl)carbamate(14)

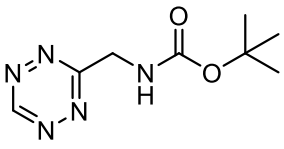

To a 25 mL schlenk tube equipped with a stir bar, formamidine acetate (1.04 g, 10 mmol), tert-butyl (cyanomethyl)carbamate (1.56 g, 10 mmol), zinc triflate(180 mg, 0.5 mmol), hydrazine hydrate(2.5 mL, 50 mmol) and DMF (2 mL) was added. The tube was sealed and heated in an oil bath at 70°C for 3 hours. After reaction, the mixture was cooled to room temperature and transferred into an Erlenmeyer flask. Sodium nitrite (6.9 g, 100 mmol) in 30 mL of water was added and followed by slow addition of 1M HCl at 0℃ until the pH value ≈ 3. (Caution! Toxic nitrogen oxide gasses generated.) The mixture was extracted with CH_2Cl_2 (3×30 mL) and the organic phase was dried over anhydrous sodium sulfate and filtered. The solvent was removed using rotary evaporation and the residue was further purified by silica column chromatography eluting with Et_2O/DCM(1:25 to 1:20). The product was obtained as a red purple solid (198 mg, 9%). ^{1}H NMR (400 MHz, Chloroform-*d*) δ 10.27 (s, 1H), 5.58 (s, 1H), 5.01 (d, *J* = 5.9 Hz, 2H), 1.45 (s, 9H). HRMS-ESI (m/z) [M+H]+: Calcd. for $C_8H_{14}O_2N_5$+ 212.1142, found 212.1144.

(1,2,4,5-tetrazin-3-yl)methanamine(15)

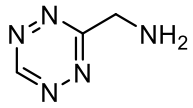

In a 100 mL round-bottom flask, compound **14** (80 mg, 0.38 mmol) was dissolved in DCM (2 mL) and Trifluoroacetic acid (2 mL) was added, and the mixture was left stirring at rt for 0.5 h. The volatiles were removed under reduced pressure and the remaining residue was suspended in toluene. The solvent was evaporated and the procedure was repeated two more times. The pink solid was collected and dried under vacuum to yield compound **15** in quantitative yield as an orange solid. The crude material was considered pure enough for subsequent reactions and the identity was confirmed by HRMS-ESI (m/z) [M+H]+: Calcd. for $C_3H_6N_5$+ 112.0618, found 112.0622.The crude was used directly without further purification.

5-(3-((1,2,4,5-tetrazin-3-yl)methyl)thioureido)-2-(6-hydroxy-3-oxo-3H-xanthen-9-yl)benzoic acid(Tz-FL-S)

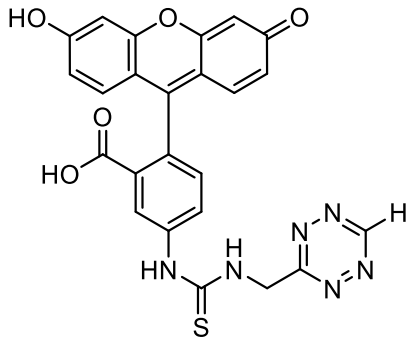

Compond **15** (34 mg, 0.3 mmol) was taken into a 25 mL round-bottom flask and dissolved in 2 mL anhydrous DMF, followed by addition of fluorescein-5-isothiocyanate (compound **12**, 119 mg, 0.3 mmol) and DIPEA (130 μL, 0.75 mmol). The reaction mixture was stirred in the dark at room temperature for 1 h and then concentrated in vacuo. The crude product was purified by preparation thin layer chromatography with DCM : MeOH = 10 : 1. The product was obtained as a red orange solid (47 mg, 31%). For further purification, methanol was used to dissolve the product and injected into HPLC. (Method used: solvent A: H_2O + 0.1% HCOOH; solvent B: CH_3CN; gradient: 10% B → 90% B in 25 min, then 95% B for 5 min and 5% B for 5 min). The product eluates at 18.5 min (on a Shiseido® C18 column (5 μm, 250 × 10 mm) at 4.7 mL/min flow rate). ^{1}H NMR (400 MHz, Methanol-d_4) δ 10.35 (s, 1H), 8.18 (s, 1H), 7.83 (d, *J* = 8.2 Hz, 1H), 7.18 (d, *J* = 8.3 Hz, 1H), 6.71 – 6.64 (m, 4H), 6.54 (dd, *J* = 8.8, 2.4 Hz, 2H), 5.44 (s, 2H). ^{13}C NMR (101 MHz, Methanol-d_4) δ 184.12, 171.28, 171.10, 159.65, 154.23, 142.08, 132.08, 130.34, 125.95, 120.36, 113.72, 111.47, 103.53. HRMS (m/z) [M+H]+: Calcd. for $C_{24}H_{17}O_5N_6S$+ 501.0976, found 501.0985.

1.3 Theoretical calculations

Quantum chemical calculations were performed using the *Gaussian16* program package.[3] The density functional theory (DFT) and time-dependent DFT (TD-DFT) calculations were conducted in the gas phase.[4,5] The geometries of the ground were optimized using PBE0-D3/6-31G* level[6–10] and excited states were optimized using CAM-B3LYP/def-TZVP level[11–13]. The hole-electron analyses were performed and visualized using Multiwfn and VMD software.[14–17]

1.4 UV-vis absorption and emission spectra

The DMSO stock solution of **Tz-CY, Tz-NA, Tz-FL** and **Tz-FL-S** was diluted to a final concentration of 10 μM in PBS buffer (pH 7.4, containing 1% DMSO as co-solvent). **TCO-D-Ala** was added at a final concentration of 90 μM when needed and reacted at room temperature for 15 min. For a turn-on fluorescence of **Tz-NA**, it was let to react with **TCO-D-Ala** in DMSO at a final concentration of 1 mM and 9 mM respectively and they were diluted 100 fold in PBS buffer (pH 7.4, 1% DMSO finally).The spectra were recorded on a Tecan Spark™ 10M Multimode Microplate Reader.

1.5 Kinetics study of reactions between TCO-D-Ala and either Tz-FL or Tz-FL-S

The kinetics of the conjugation reaction between **TCO-D-Ala** and tetrazine probes were studied by recording fluorescence intensity at 520 nm in a Tecan Spark™ 10M Multimode Microplate Reader. The data were collected after blank subtraction using PBS buffer (1×, pH 7.4, containg 1% DMSO). The reaction was performed in a 96-well plate at room temperature (25℃). The DMSO stock solution of **Tz-FL** or **Tz-FL-S** was diluted to a final concentration of 20 μM in PBS buffer (pH 7.4, containg 2% DMSO as co-solvent) as the working solution. After pipetting 100 μL working solution in the well, an equal volume of 180 μM **TCO-D-Ala** in PBS buffer was added swiftly and started monitoring. The emission intensity at 520 nm were recorded at an interval of 10 seconds. The initial points were measured with the addition of blank PBS buffer without **TCO-D-Ala**. λ_{ex} = 488 nm. The experiment was repeated three times. The kinetic data were fitted according to the equations shown below to obtain the rate constant[18]. The data were plotted with Origin 10. The fitting analyses are shown in **Fig. S3E, F** and kinetics profiles are shown in **Fig. 2C** of the main text.

Kinetics Formation:

$$\frac{dp}{dt}=k_2(C_1-p)(C_2-p) \qquad (1)$$

in which p is the product concentration and C_1 *and* C_2 are the initial starting materials' concentration respectively (C_1 = 10 μM and C_2 = 90 μM). Given that C_2 is significantly larger than C_1, to simplify kinetics fitting, the reaction is treated as a pseudo-first order reaction. C_2 is set to 80 μM (C_2*), which falls in between the initial and ending concentrations of **TCO-D-Ala**. This treatment may introduce some error; however, the order of magnitude of the rate constant will not be affected.

$$\frac{dp}{dt}=k_2C_2^*(C_1-p) \qquad (2)$$

$$\frac{d(p-C_1)}{p-C_1}=-k_2C_2^*\,dt \qquad (3)$$

$$ln\frac{p-C_1}{-C_1}=-k_2C_2^*t \qquad (4)$$

$$p=C_1-C_1e^{-k_2C_2^*t} \qquad (5)$$

Since the monitored fluorescence intensity at 520 nm is generated by the probe and its corresponding click products, there is equation **(6)**. The reaction rate constant k_2 can be obtained by fitting the equation **(7)**. F_1 and F_2 represent the fluorescence intensity of each μM probe and its corresponding product, respectively, and F represents the monitored total fluorescence intensity.

$$F=F_1(C_1-p)+F_2p \qquad (6)$$

$$F-F_1C_1=(F_2-F_1)C_1-(F_2-F_1)C_1e^{-k_2C_2^*t} \qquad (7)$$

1.6 Fluorescence stability of clicked products formed by TCO-D-Ala and Tz-FL-S

The click products were first rapidly generated by **Tz-FL-S** and **TCO-D-Ala** in a molar ratio of 1 : 9 in PBS buffer at room temperature within 5 minutes. After rapid aliquoting into two different EP tubes, the initial fluorescence intensity at the starting time point was recorded. The tubes were then placed in incubators at 30 °C and 37 °C in the dark, and fluorescence intensity was measured at 1 h, 2 h, 4 h, 8 h, 24 h, 48 h, 72 h, and 96 h.

1.7 Quantitative analysis of TCO-D-Ala uptake by *E. coli*, *B. subtilis* and *S. aureus*

For *Escherchia coli* ATCC 25922, *Bacillus subtilis* ATCC 6633, *Staphylococcus aureus* ATCC 29213, single colony was inoculated in 5 ml of their respective media (LB for *E. coli* and *B. subtilis*, TSB for *S.aureus*). The bacteria were grown at 37 ℃ and 180 rpm overnight. Then they were diluted to OD_{600} 0.05 and then grown to an OD_{600} of ~0.3 at 37 ℃ and 180 rpm. Then, **TCO-D-Ala** (0.1 M stock in H_2O) were added to the bacterial cell cultures (final concentration 0-1000 μM) and the cultures were allowed to continue growth to an OD_{600} of 1.0~1.5. They were pelleted by centrifuge at 8000 rpm for 1 min. The supernatant was removed and the pellet was resuspended in 1 mL PBS and washed once. The cell pellet was then incubated with 100 μL of 50 μM **Tz-FL-S** at 37 ℃ for 30 minutes. The cells were pelleted by centrifuge at 8000 rpm for 1 min. The supernatant was removed and the pellet was resuspended in 1 mL PBS and washed once. They were diluted with PBS and determined the OD_{600} and fluorescence intensity at 520 nm (λ_{ex} = 488 nm) in a Tecan Spark™ 10M Multimode Microplate Reader.

1.8 Confocal fluorescence imaging of bacteria peptidoglycan labeling using TCO-D-Ala with Tz-CY, Tz-NA, Tz-FL or Tz-FL-S

For *Escherchia coli* ATCC 25922, *Bacillus subtilis* ATCC 6633, *Staphylococcus aureus* ATCC 29213, single colony was inoculated in 5 ml of their respective media (LB for *E. coli* and *B. subtilis*, TSB for *S.aureus*). The bacteria were grown at 37 ℃ and 180 rpm

overnight. Then they were diluted to OD_{600} 0.05 and transferred into two culture tubes as treatment groups and negative control groups in 1 mL per tube. The treatment groups were added 1 mM of **TCO-D-Ala** (0.1 M stock in H_2O), while negative control groups were not. When grown to an OD_{600} of 0.4~0.6 (it takes about three doubling times) at 37 ℃ and 180 rpm, the bacteria were then transferred into the EP tubes. They were pelleted by centrifuge at 8000 rpm for 1 min. The supernatant was removed and the pellet was resuspended in 1 mL PBS. The wash process was repeated twice for both treatment groups and negative control groups. For each group, the cells were devided into four aliquots respectively and incubated in 100 μL PBS with 10 μM corresponding probe (1 mM stock in DMSO) as well as 20 μg/mL Hoechst 33342 standing at 37 °C in dark for 1 h. The cells were washed twice with PBS and resuspened in 20 μL PBS to be used for fluorescence imaging. For Hoechst 33342, λ_{ex} = 405 nm, λ_{em} = 422-468 nm (false-colored blue). For **Tz-CY**, λ_{ex} = 640 nm, λ_{em} was collected using a 800 nm long-pass edge filter (false-colored red). For **Tz-NA**, λ_{ex} = 488 nm, λ_{em} = 565-605 nm (false-colored green). For **Tz-FL** and **Tz-FL-S**, λ_{ex} = 488 nm, λ_{em} = 505-548 nm (false-colored green). For each strain and each probe, images of the treatment group and the negative control group were collected under the same imaging conditions, and processed equally by ImageJ.

1.9 MIC assay

The MIC values were defined as the lowest concentration of the drug necessary to inhibit bacterial growth. Each bacterial strain was incubated in the required broths with different concentrations of compounds in a 96-well plate for 24 h. The MIC values were determined from OD_{600} values in three separate experiments. The OD_{600} values of the wells in the absence of bacteria were used as the control.

1.10 Confocal fluorescence imaging of bacteria L-form conversion

For *Escherchia coli* ATCC 25922, *Bacillus subtilis* ATCC 6633, *Staphylococcus aureus* ATCC 29213 and *Staphylococcus aureus* RN 4220, single colony was inoculated in 5 ml of their respective media (LB for *E. coli* and *B. subtilis*, TSB for *S.aureus*). The bacteria were grown at 37 ℃ and 180 rpm overnight. Then they were diluted to OD_{600} 0.05 and added 1 mM of **TCO-D-Ala** (0.1 M stock in H_2O). When grown to an OD_{600} of 0.4~0.6 (it takes about three doubling times) at 37 ℃ and 180 rpm, 1 mL of the bacteria were then transferred into the EP tubes. They were pelleted by centrifuge at 8000 rpm for 1 min. The supernatant was removed and the pellet was resuspended in 1 mL PBS. The wash process was repeated twice. Then the cells were incubated with 10 μM **Tz-FL-S** (1 mM stock in DMSO) as well as 20 μg/mL Hoechst 33342 in 500 μL PBS standing at 37 °C in dark for 1 h. The cells were washed twice with PBS and resuspened in 500 μL NB/MSM medium. After adding the corresponding antibiotics, the bacteria were incubated at 30 °C and monitored through sampling and imaging by the confocal laser scanning microscope with 60 × magnification. For *S. aureus* ATCC 29213, 400 μg/mL fosfomycin was added and 24 hours were taken to monitor. For *S. aureus* RN 4220, 200 μg/mL penicillin G and 2 μg/mL lysostaphin were added, and 2 hours were taken to monitor. For *B. subtilis* ATCC 6633, 200 μg/mL penicillin G and 100 μg/mL lysozyme were added, and 3 hours were taken to monitor. For *E. coli* ATCC 25922, 100 μg/mL fosfomycin and 100 μg/mL penicillin G were added, and 2 hours were taken to monitor. For Hoechst 33342, λ_{ex} = 405 nm, λ_{em} = 422-468 nm (false-colored blue). For **Tz-FL-S**, λ_{ex} = 488 nm, λ_{em} = 505-548 nm (false-colored green). For each strain, respectively, the green fluorescence images at different time points were collected under the same imaging conditions, and processed equally by ImageJ.

1.11 Confocal fluorescence imaging of bacteria induced by different antibiotics

For *Staphylococcus aureus* ATCC 29213, single colony was inoculated in 5 ml of TSB. The bacteria were grown at 37 ℃ and 180 rpm overnight. Then they were diluted to OD_{600} 0.05 and added 1 mM of **TCO-D-Ala** (0.1 M stock in H_2O). When grown to an OD_{600} of 0.4~0.6 (it takes about three doubling times) at 37 ℃ and 180 rpm, 2 mL of the bacteria were then transferred into the EP tubes. They were pelleted by centrifuge at 8000 rpm for 1 min. The supernatant was removed and the pellet was resuspended in 1 mL PBS. The wash process was repeated twice. Then the cells were incubated with 10 μM **Tz-FL-S** (1 mM stock in DMSO) as well as 20 μg/mL Hoechst 33342 in 1 mL PBS standing at 37 °C in dark for 1 h. The cells were washed twice with PBS and resuspened in 2 mL of NB/MSM medium. Then the cells were devided into fourteen aliquots and incubated with corresponding antibiotics at a concentration of 10× MIC at 30 °C. After 24 h, they were sampled and imaged by the confocal laser scanning microscope with 60 × magnification. For Hoechst 33342, λ_{ex} = 405 nm, λ_{em} = 422-468 nm (false-colored blue). For **Tz-FL-S**, λ_{ex} = 488 nm, λ_{em} = 505-548 nm (false-colored green). For each treatment, the green fluorescence was collected under the same imaging conditions, and processed equally by ImageJ.

1.12 Confocal fluorescence imaging of drug-susceptible and drug-resistant *S. aureus* L-form conversion

For *Staphylococcus aureus* ATCC 29213 (methicillin-susceptible strain) and *Staphylococcus aureus* ATCC 33592 (methicillin-resistant strain), single colony was inoculated in 5 ml of TSB (for ATCC 29213) or NB (for ATCC 33592). The bacteria were grown at 37 ℃ and 180 rpm overnight. Then they were diluted to OD_{600} 0.05 and added 1 mM of **TCO-D-Ala** (0.1 M stock in H_2O). When grown to an OD_{600} of 0.4~0.6 (it takes about three doubling times) at 37 ℃ and 180 rpm, 1 mL of the bacteria were then transferred into the EP tubes. They were pelleted by centrifuge at 8000 rpm for 1 min. The supernatant was removed and the pellet was resuspended in 1 mL PBS. The wash process was repeated twice. Then the cells were incubated with 10 μM **Tz-FL-S** (1 mM stock in DMSO) as well as 20 μg/mL Hoechst 33342 in 500 μL PBS standing at 37 °C in dark for 1 h. The cells were washed twice with PBS and resuspened in 1 mL of NB/MSM medium. For the treatment in liquid condition, the cells were incubated with ampicillin at a concentration of 10× or 50× MIC respectively at 30 °C. They were sampled and imaged by the confocal laser scanning microscope with 60 × magnification. For bacteria induced by solid agar, 1~2 μl cells were firstly placed on 35 mm sterile glass bottom microwell dishes and then a thin layer of 50× MIC ampicillin-contained NB/MSM with 1% agar was placed on the top of the dishes. They were incubated and imaged at 30 °C. For Hoechst 33342, λ_{ex} = 405 nm, λ_{em} = 422-468 nm (false-colored blue). For **Tz-FL-S**, λ_{ex} = 488 nm, λ_{em} = 505-548 nm (false-colored green). For each strain, respectively, the green fluorescence images at different time points were collected under the same imaging conditions, and processed equally by ImageJ.

2. Results and Discussion

2.1 Absorbance spectral responses and HRMS spectra of Tz-CY, Tz-NA,Tz-FL reacting with TCO-D-Ala

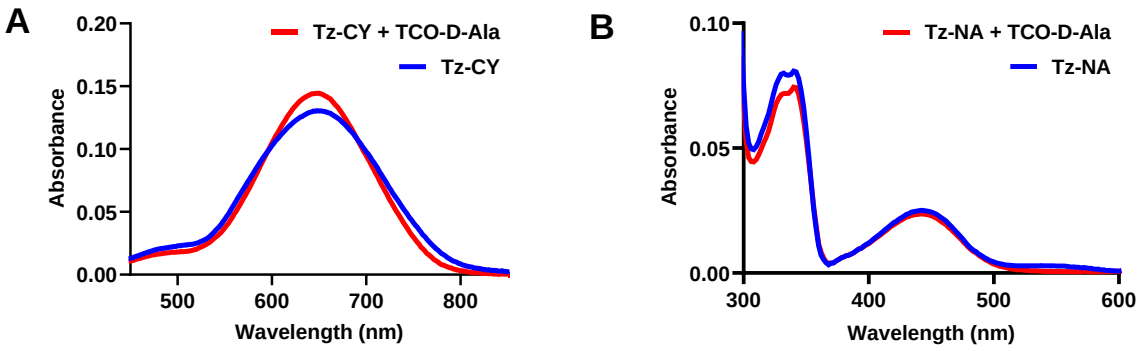

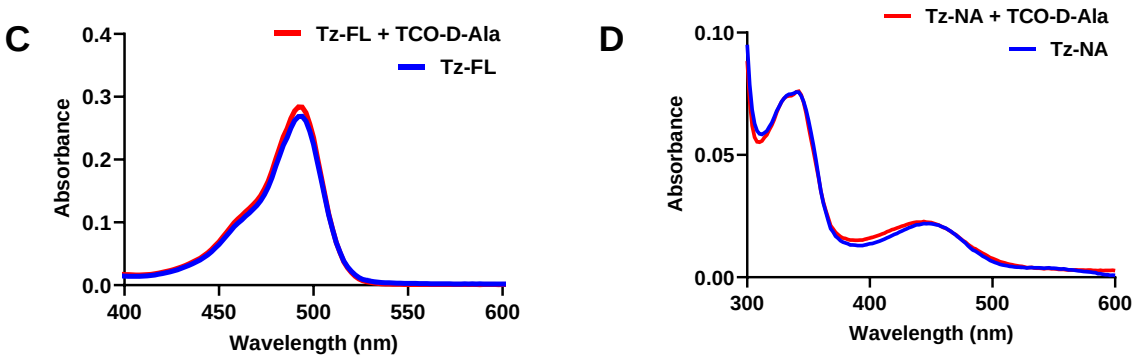

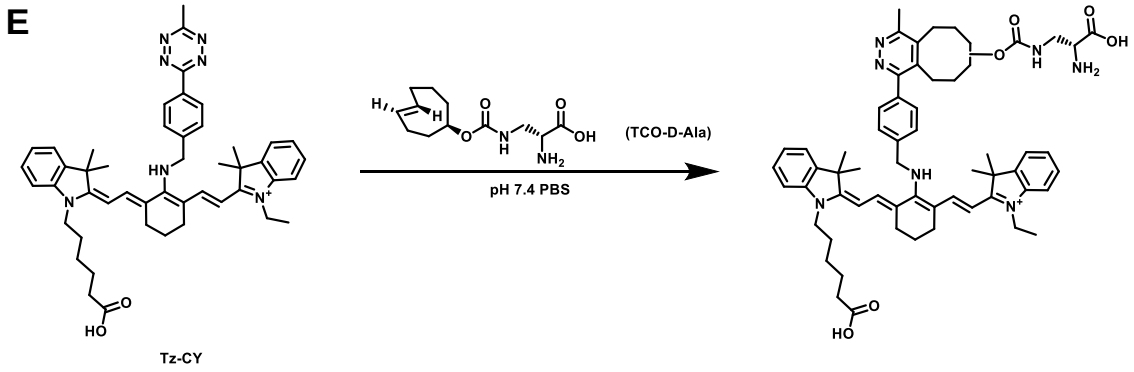

[M]+ Calcd. 988.5695

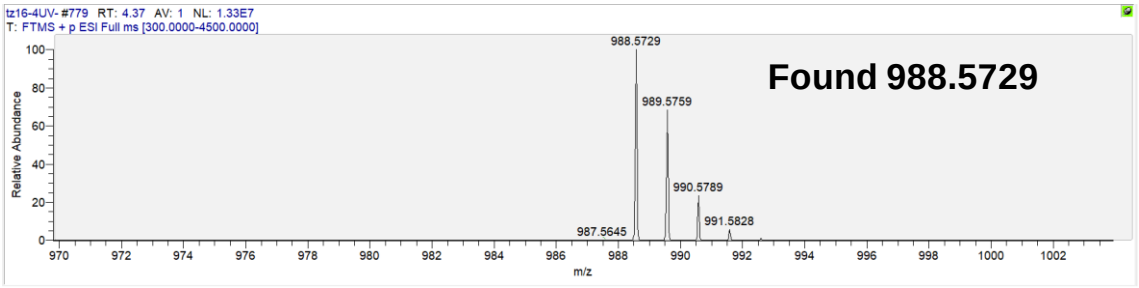

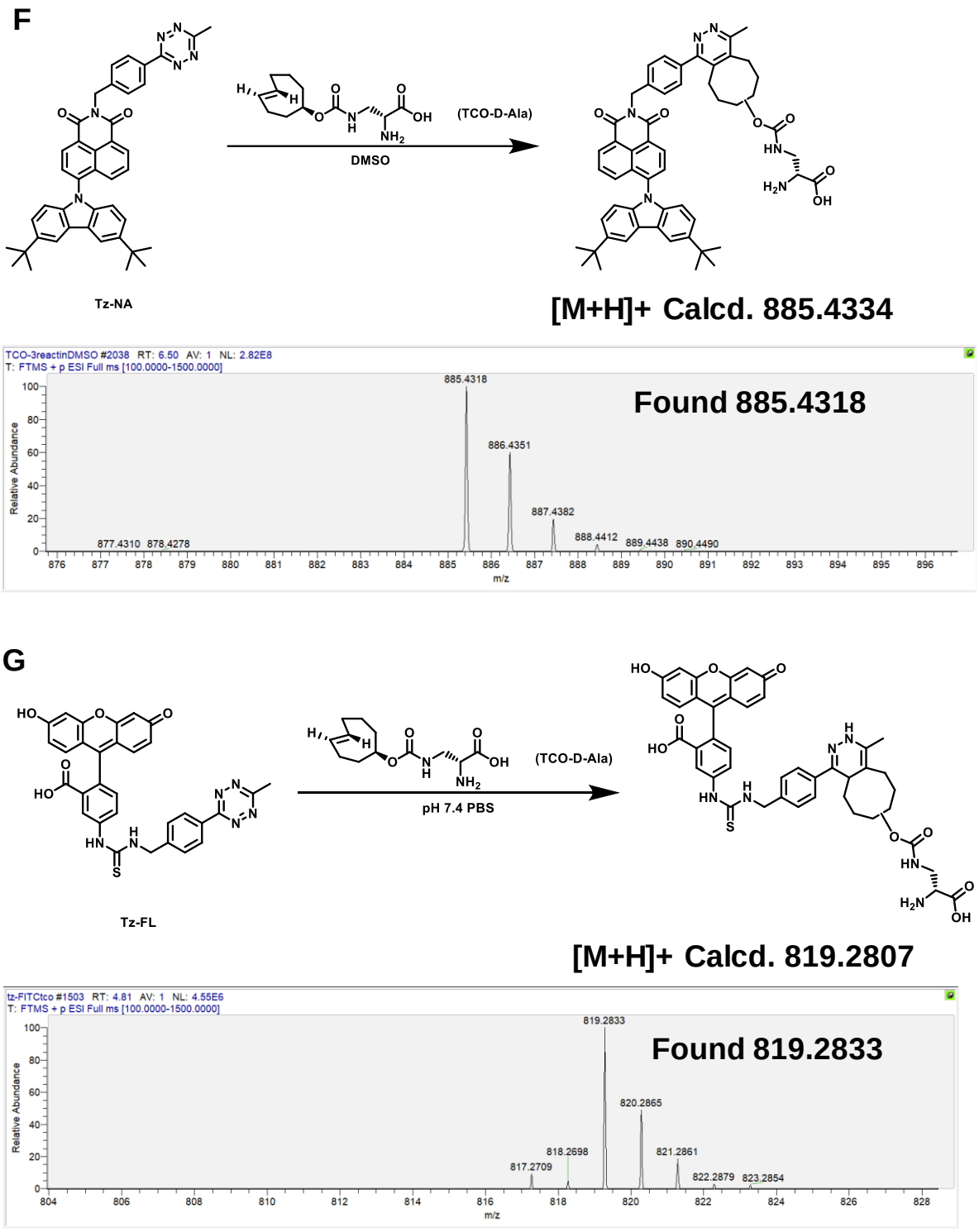

Fig. S1. The absorbance intensity changes of 10 μM **Tz-CY** (A), **Tz-NA** (B), **Tz-FL** (C) in PBS (1% DMSO). (D) The fluorescence intensity changes of 10 μM **Tz-NA** reacting with 90 μM **TCO-D-Ala** in PBS (1% DMSO). (E), (F), and (G) High-resolution mass spectrometry detected the expected product after the reaction of **Tz-CY**, **Tz-NA**, **Tz-FL** with **TCO-D-Ala**.

2.2 Confocal fluorescence imaging of bacteria peptidoglycan labeling using TCO-D-Ala with Tz-CY, Tz-NA, Tz-FL

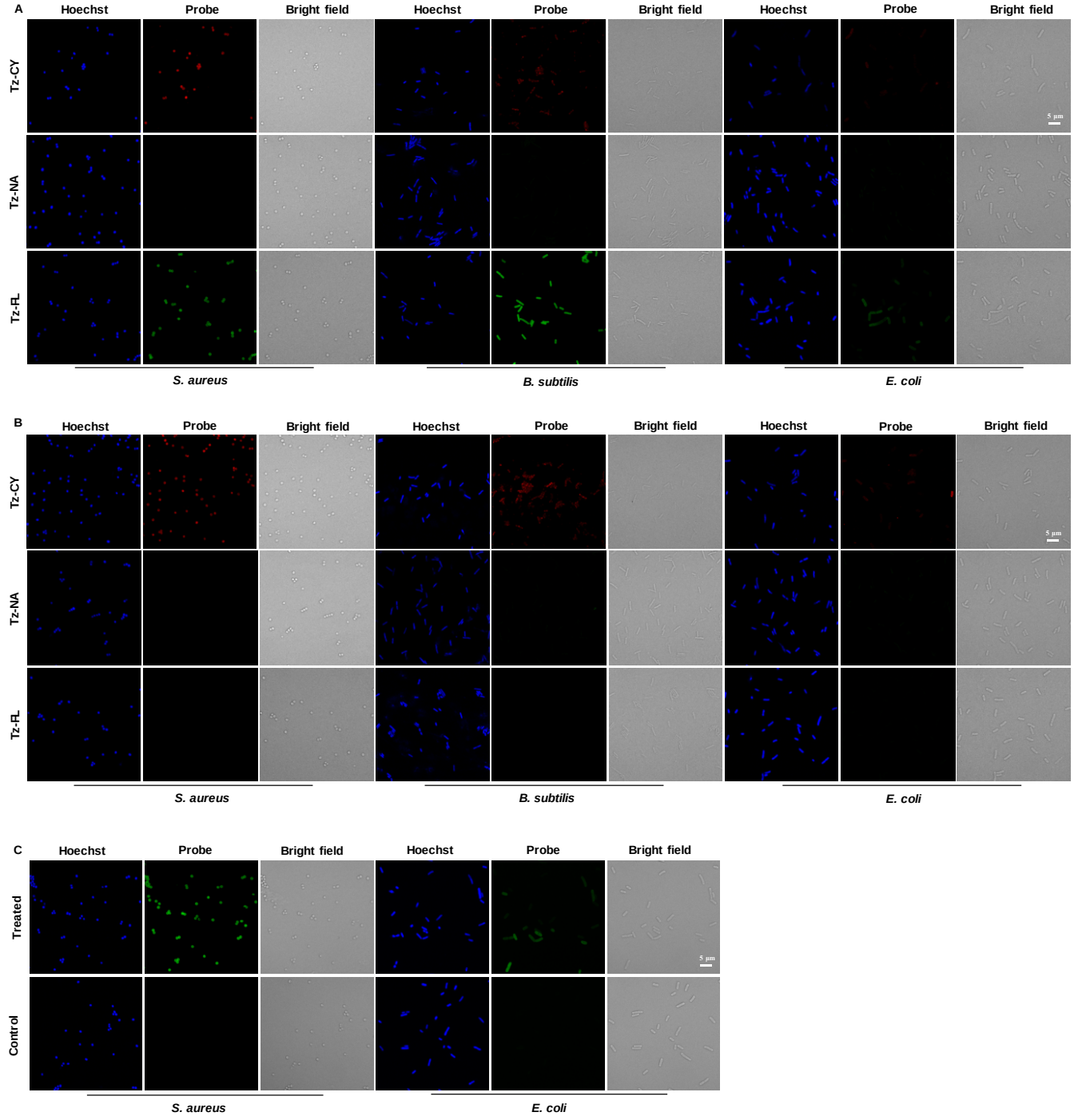

Fig. S2. Use **TCO-D-Ala** and **Tz-CY**, **Tz-NA** and **Tz-FL** to label the *Staphylococcus aureus* ATCC 29213, *Bacillus subtilis ATCC* 6633, *Escherichia coli* ATCC 25922 and capture the images of treated group (A) and negative control group (B). For detailed methods, see Experimental procedures 1.8. (C) Additional images captured using **Tz-FL** to label *Staphylococcus aureus* ATCC 29213 and *Escherichia coli* ATCC 25922. Scale bar: 5 μm.

3.3 Property characterization of Tz-FL-S

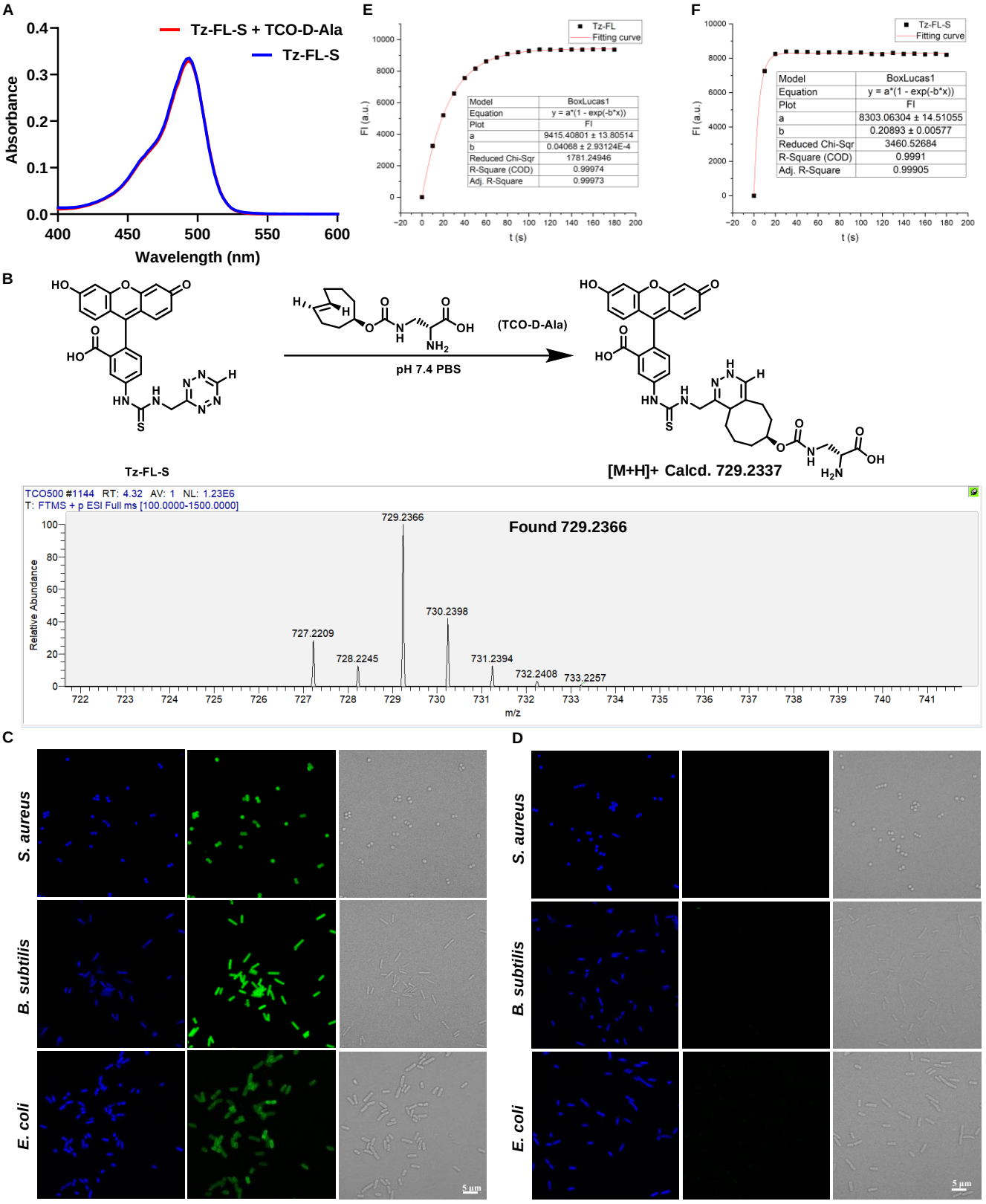

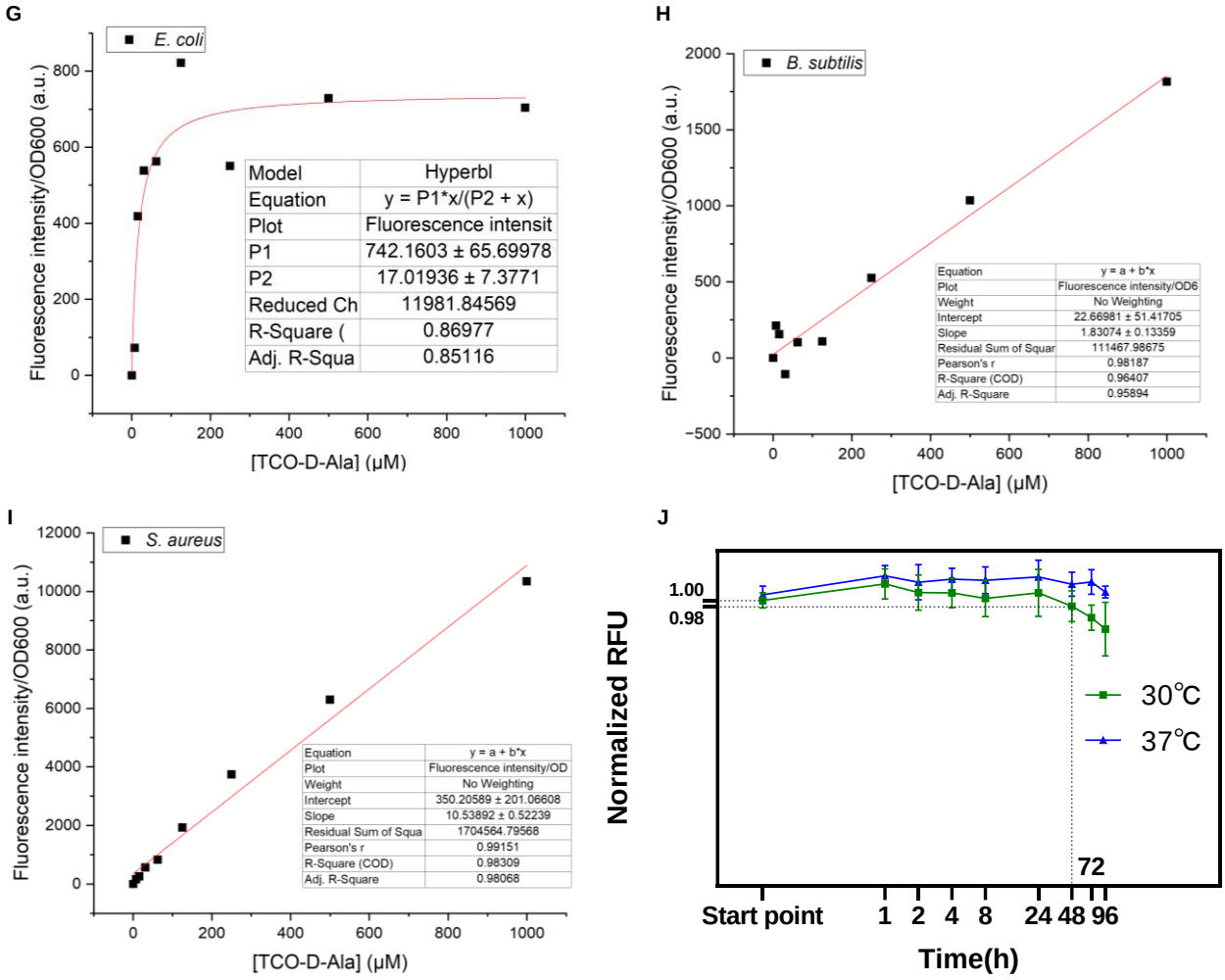

Fig. S3. (A) The absorbance intensity changes of 10 μM **Tz-FL-S** reacting with 90 μM **TCO-D-Ala** in PBS (1% DMSO). (B) High-resolution mass spectrometry detected the expected product after the reaction of **Tz-FL-S**. (C) The corresponding images including Hoechst 33342 staining and bright field in the treated group (**Fig. 2d**) of different strains labeled with **Tz-FL-S** and (D) Images of the negative control group of different strains labeled with **Tz-FL-S**. For detailed methods, see Experimental procedures 2.6. Scale bar: 5 μm. (E) and (F) show the curve fitting and analyses of knetics of **Tz-FL** and **Tz-FL-S** respectively. Fitting the kinetic data according to the equation **(7)** in Experimental procedures 1.5 gives the k_2 value. $FI = F\text{-}F_1C_1$, where F and F_1C_1 respectively equal to each fluorescence intensity data and the fluorescence intensity data (t = 0 s) represented in **Fig. 2C** in the main text. Concentration profiles of **TCO-D-Ala** incorporation into *E. coli* (G) , *B. subtilis* (H) and *S. aureus* (I). The data were fit to a hyperbolic curve for *E. coli* and a linear fit for *B.subtilis* and *S. aureus*. The data were fitted according to Michaelis-Menten kinetics as discussed in the main text. (J) Fluorescence stability of clicked products formed by **Tz-FL-S** and **TCO-D-Ala** under 30℃ and 37℃.

3.4 Theoretical calculations of ETDS on Tz-FL and Tz-FL-S

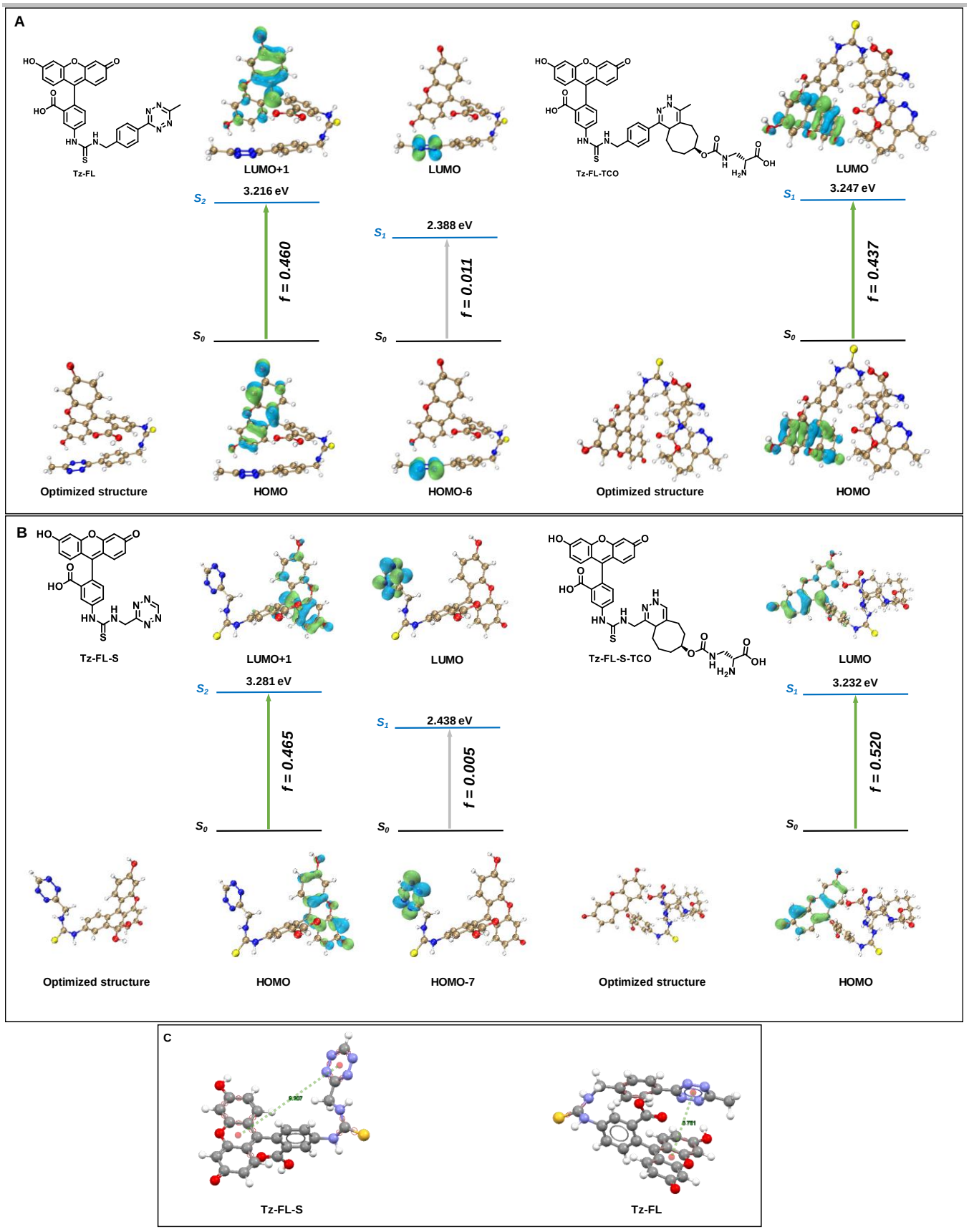

Fig. S4. Molecular structures, optimized geometries, and vertical excitation energies (VES) of various excited states, corresponding oscillator strength (*f*), and dominating frontier molecular orbitals involved during these transitions of (A) **Tz-FL** and **Tz-FL-TCO,** (B) **Tz-FL-S** and **Tz-FL-S-TCO**. (C)The distance between the centroids of tetrazine ring and the fluorophores in the optimized geometries of **Tz-FL-S** and **Tz-FL** is 9.207 Å and 5.751 Å, respectively.

3.5 Minimal Inhibitory Concentrations (MIC) for *S.aureus*

Antibiotics	MIC (μg/mL)	Antibiotics	MIC (μg/mL)
	S. aureus ATCC 29213		*S. aureus* ATCC 33592
Fosfomycin	4	Ampicillin	128
Ampicillin	2		
Penicillin G	2		
Cefoperazone	4		
Meropenem	0.12		
Linezolid	4		
Azithromycin	2		
Clindamycin	0.25		
Amikacin	4		
SMZ+TMP(19:1)	9.5+0.5		
TMP	4		
Levofloxain	1		
Rifamycin	0.016		
Vancomycin	2		

Table S1. Minimal Inhibitory Concentrations (MIC) of different antibiotics for *S.aureus* ATCC 29213 and ampicillin for *S.aureus* ATCC 33592**.**

3.6 Confocal fluorescence imaging of bacteria induced by fosfomycin and TMP

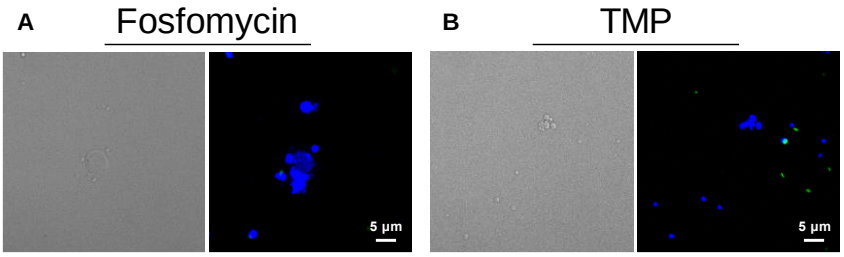

Fig. S5. The representative images of CWDB observation inducing *S. aureus* ATCC 29213 by treatment of fosfomycin (A) and TMP (B) at a concentration of 10× MIC for 24 h. Scale bar: 5μm.

3.7 Quantitative analysis of the cell-wall deficient bacteria across different antibiotic treatments

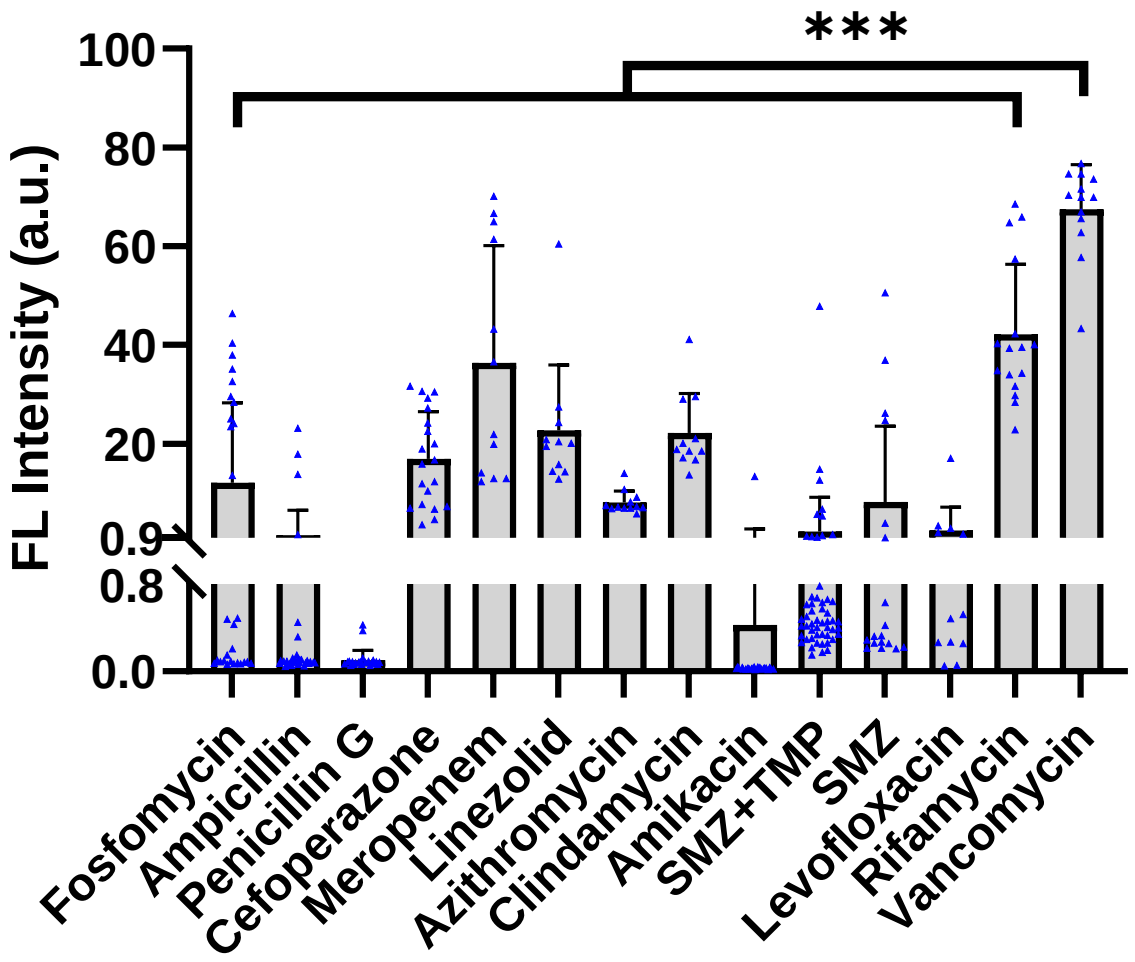

Fig. S6. Quantitative analysis for confocal fluorescence images of CWDB formation in *S. aureus* ATCC 29213 after treatment with various inducers**.** The data were obtained by using ImageJ to quantify the mean fluorescence intensity of individual bacteria in multiple images collected after treatment with different antibiotics ($n > 10$). When comparing the fluorescence intensities of bacteria treated with different antibiotics to those treated with vancomycin, which exhibited the least reduction in peptidoglycan signal, all other antibiotic treatments resulted in significantly lower fluorescence intensities. Data are represented as mean + SD and analyzed using a two-tailed Mann–Whitney *U* test. ***$P < 0.001$.

3.7 Confocal fluorescence imaging of drug-susceptible and drug-resistant *S. aureus* L-form conversion

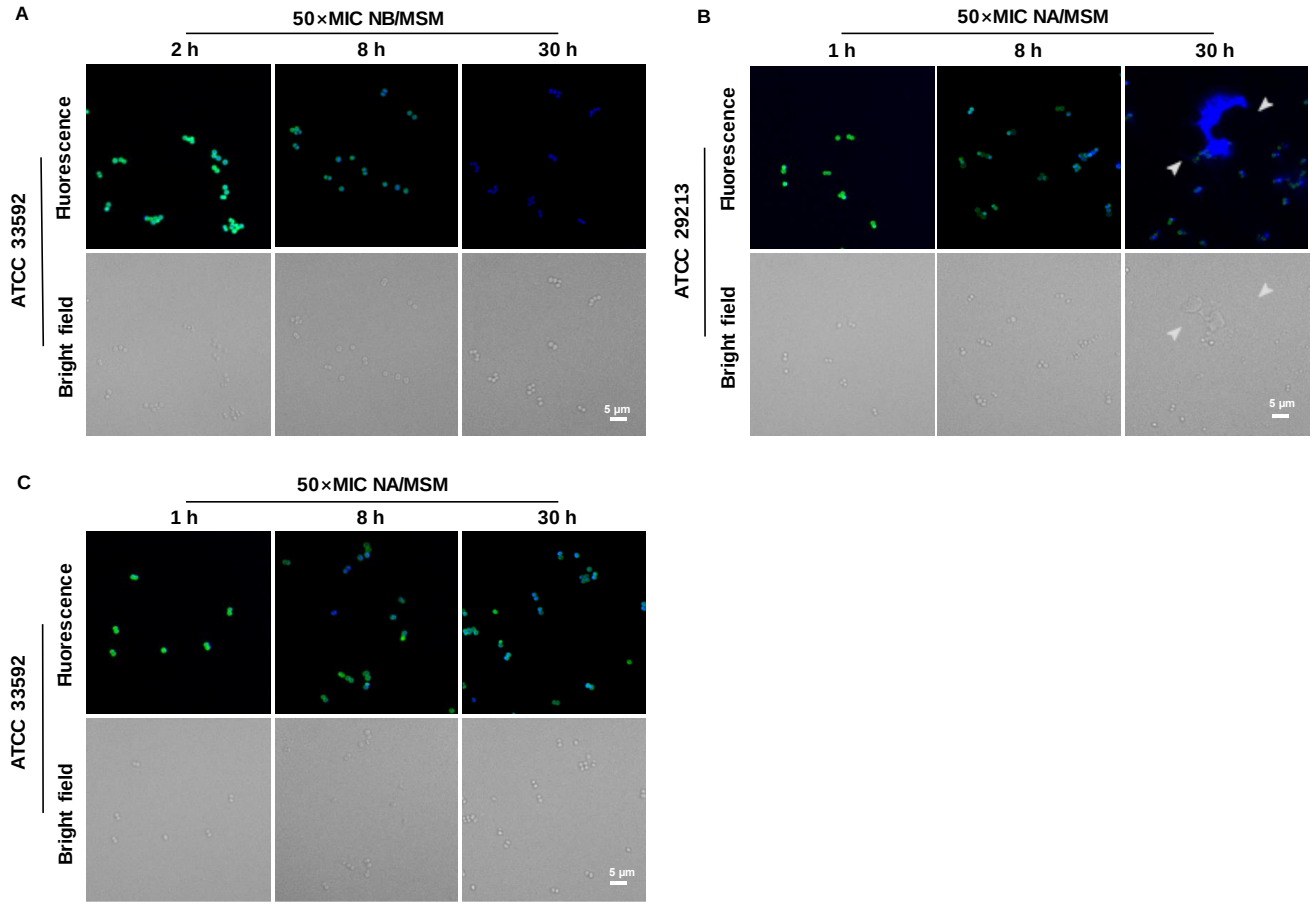

Fig. S7. Fluorescence images monitoring the L-form conversion processes of drug-resistant and drug-susceptible *Staphylococcus aureus* induced by ampicillin. (A) The drug-resistant strain ATCC 33592 was induced by ampicillin at 50 × MIC in NB/MSM medium at 30 °C for 30 h. (B) The drug-susceptible strain ATCC 29213 was induced by ampicillin at 50 × MIC on NA/MSM medium at 30 °C for 30 h. (C) The drug-resistant strain ATCC 33592 was induced by ampicillin at 50 × MIC on NA/MSM medium at 30 °C for 30 h. The rows of “Fluorescence” show the merged fluorescence images. Grey arrow : distinctly inflated CWDB with complete loss of cell wall. Scale bar : 5 μm.

4. Copies of NMR spectra

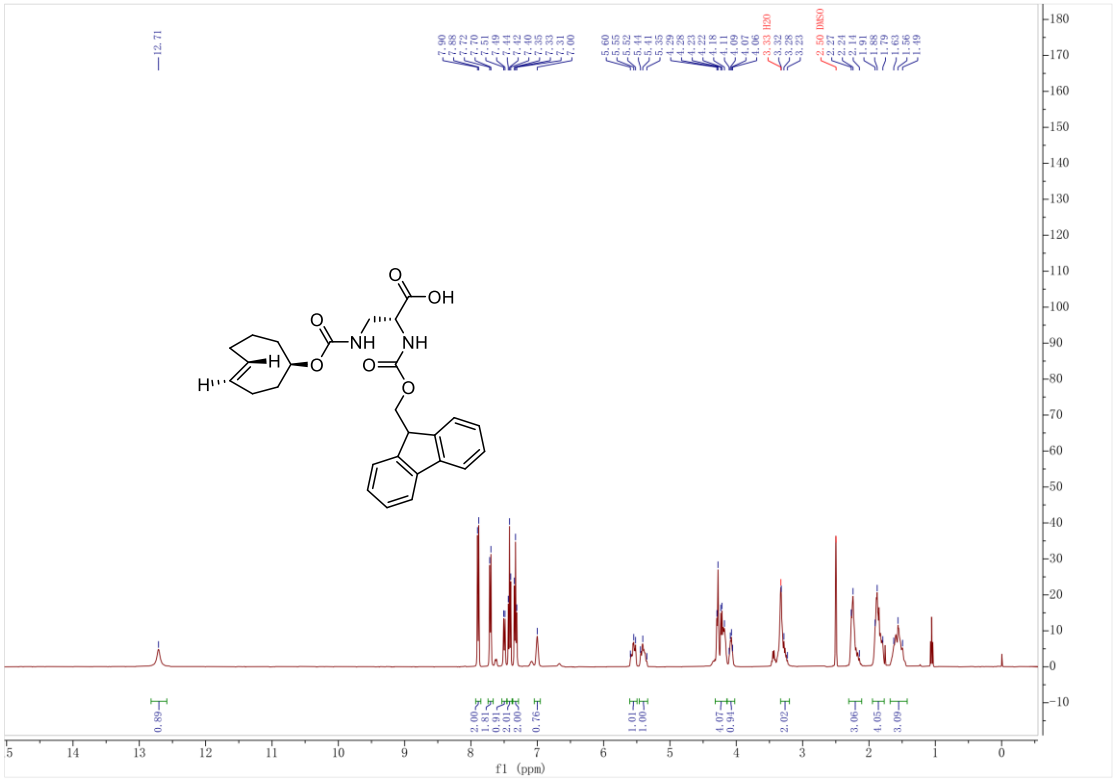

^{1}H NMR (400 MHz, DMSO-d_6) of compound (2)

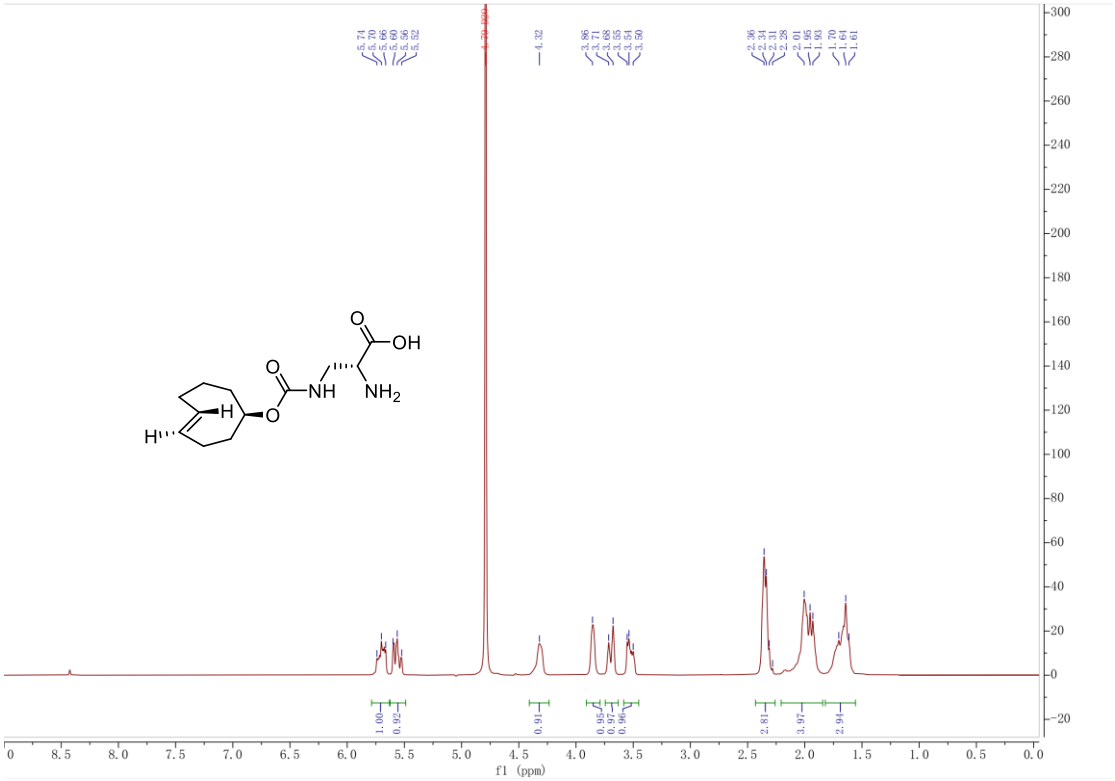

^{1}H NMR (400 MHz, Deuterium Oxide) of **TCO-D-Ala**

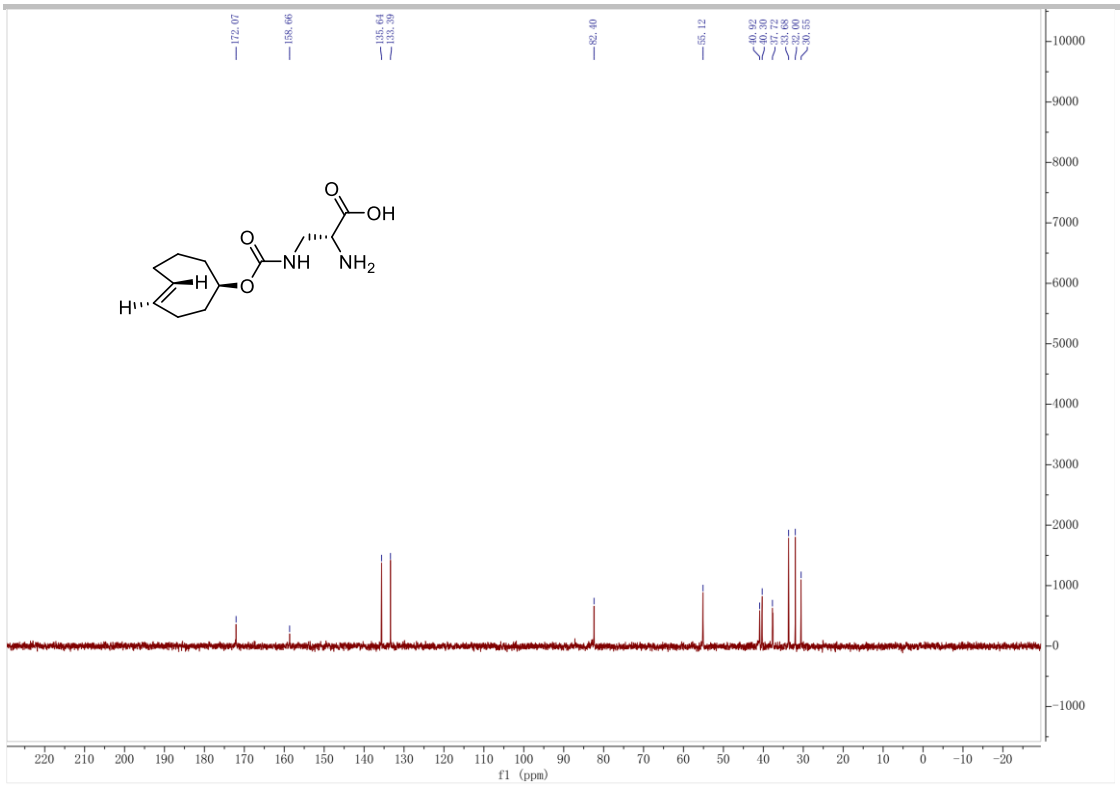

^{13}C NMR (101 MHz, Deuterium Oxide) of **TCO-D-Ala**

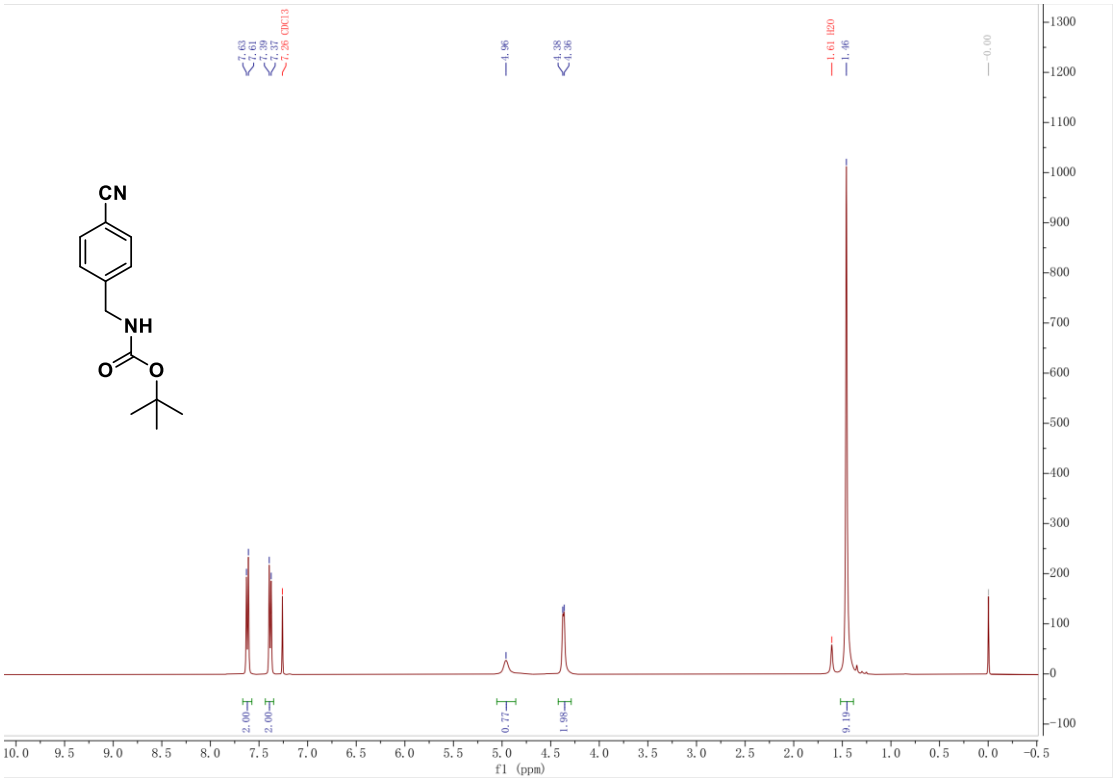

^{1}H NMR (400 MHz, Chloroform-*d*) of compound (4)

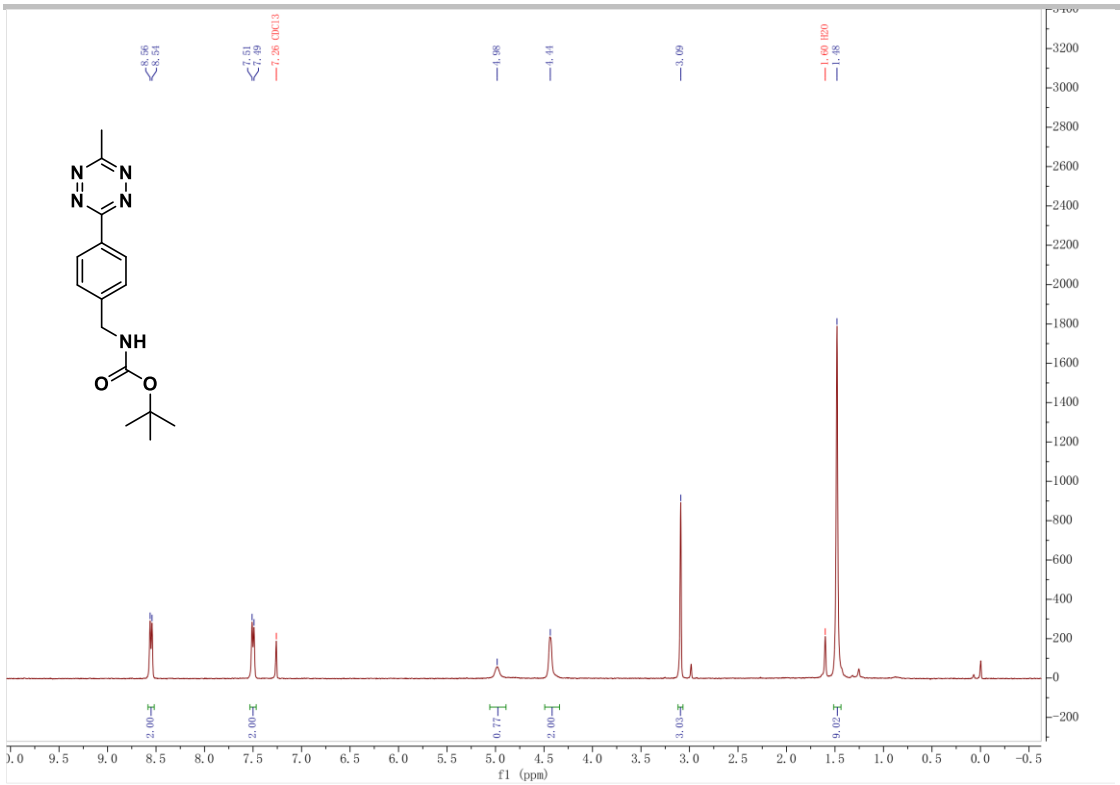

^{1}H NMR (400 MHz, Chloroform-*d*) of compound (5)

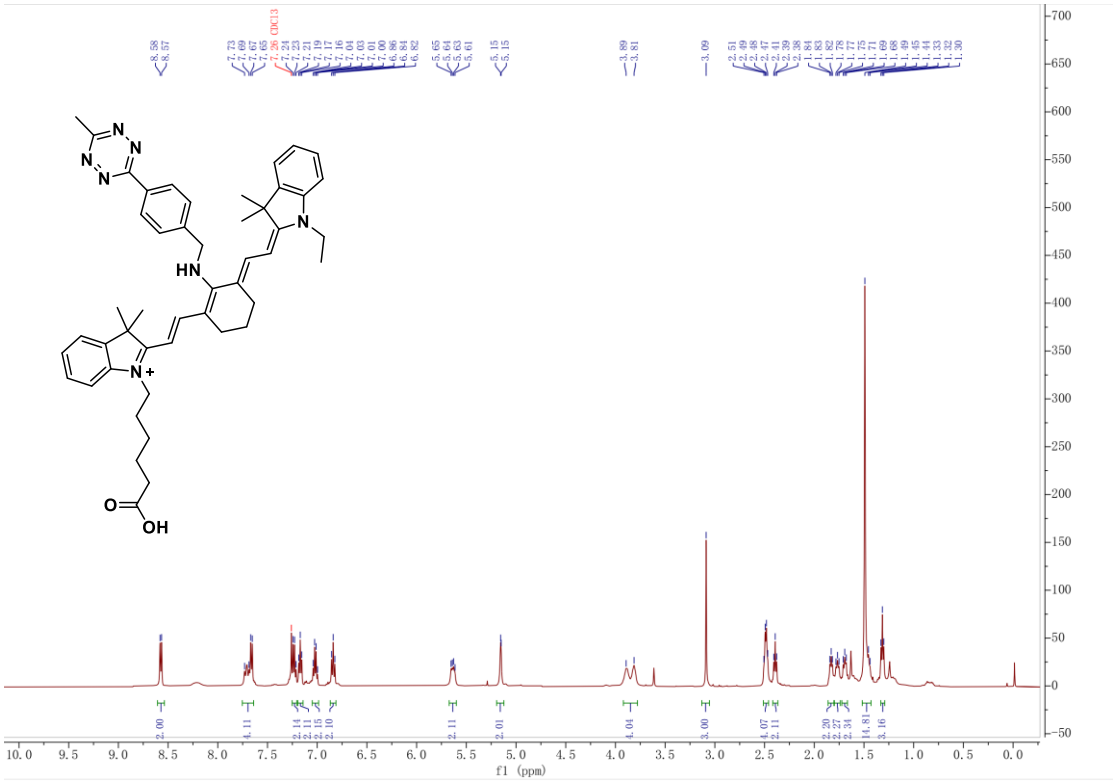

^{1}H NMR (500 MHz, Chloroform-*d*) of **Tz-CY**

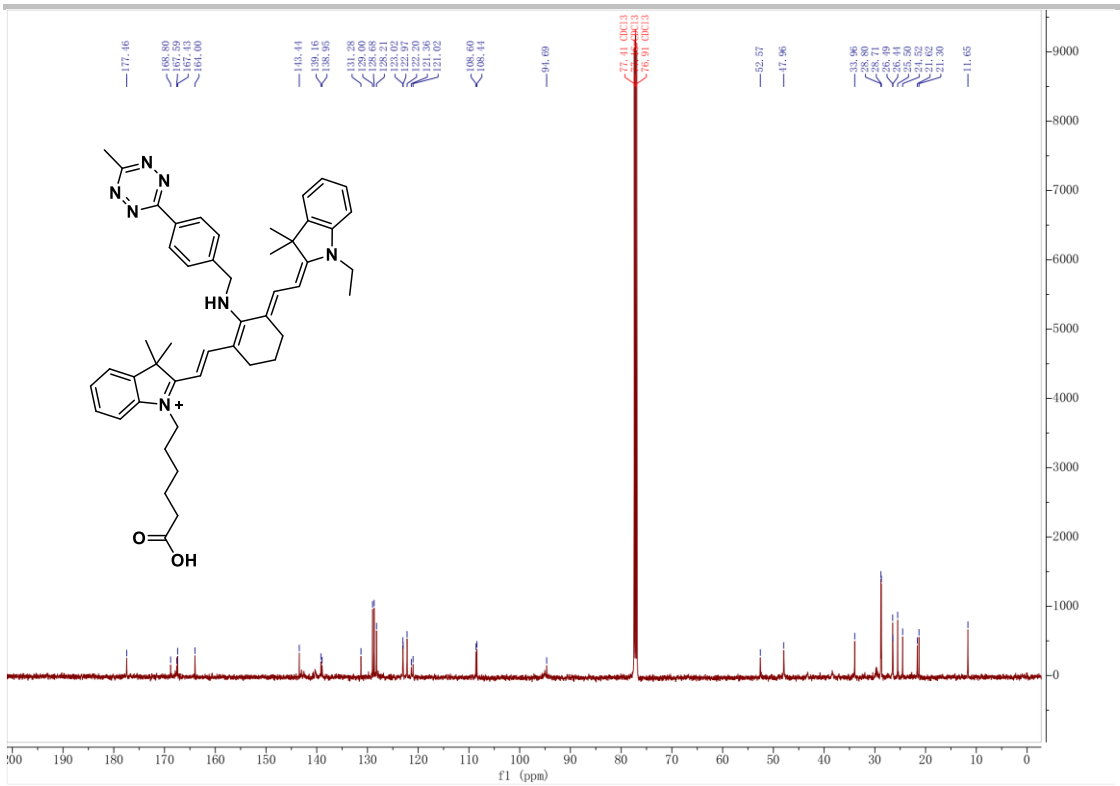

^{13}C NMR (126 MHz, Chloroform-*d*) of **Tz-CY**

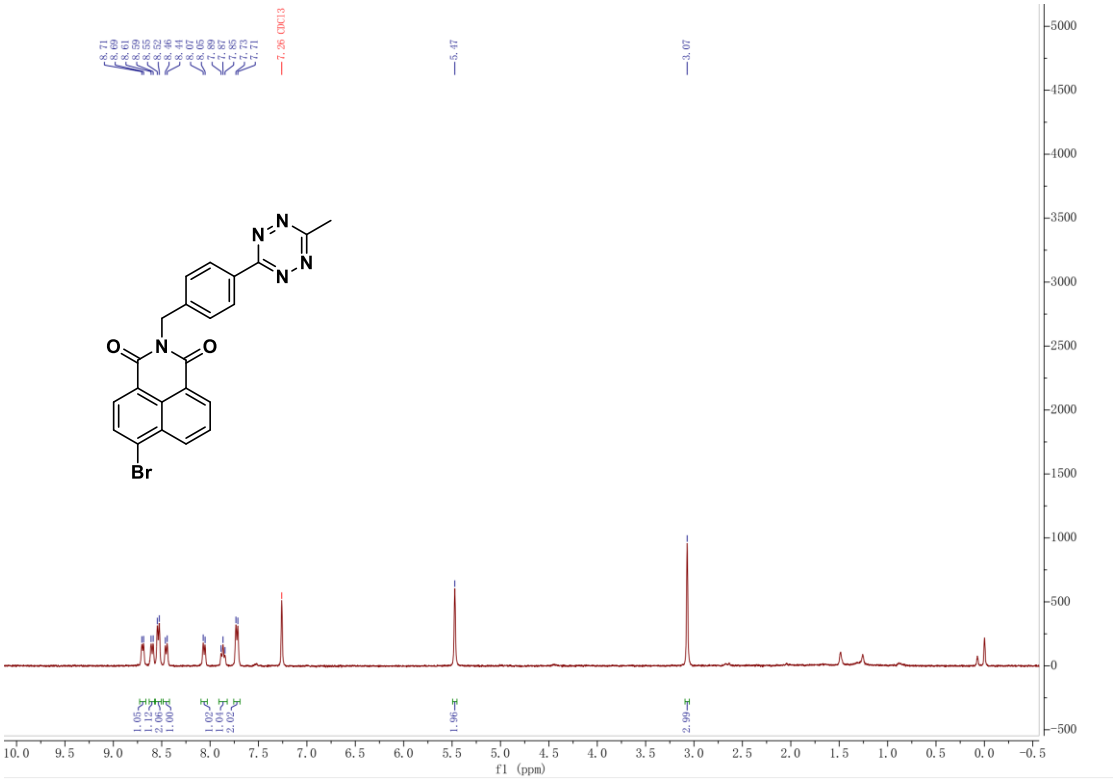

^{1}H NMR (400 MHz, Chloroform-*d*) of compound (10)

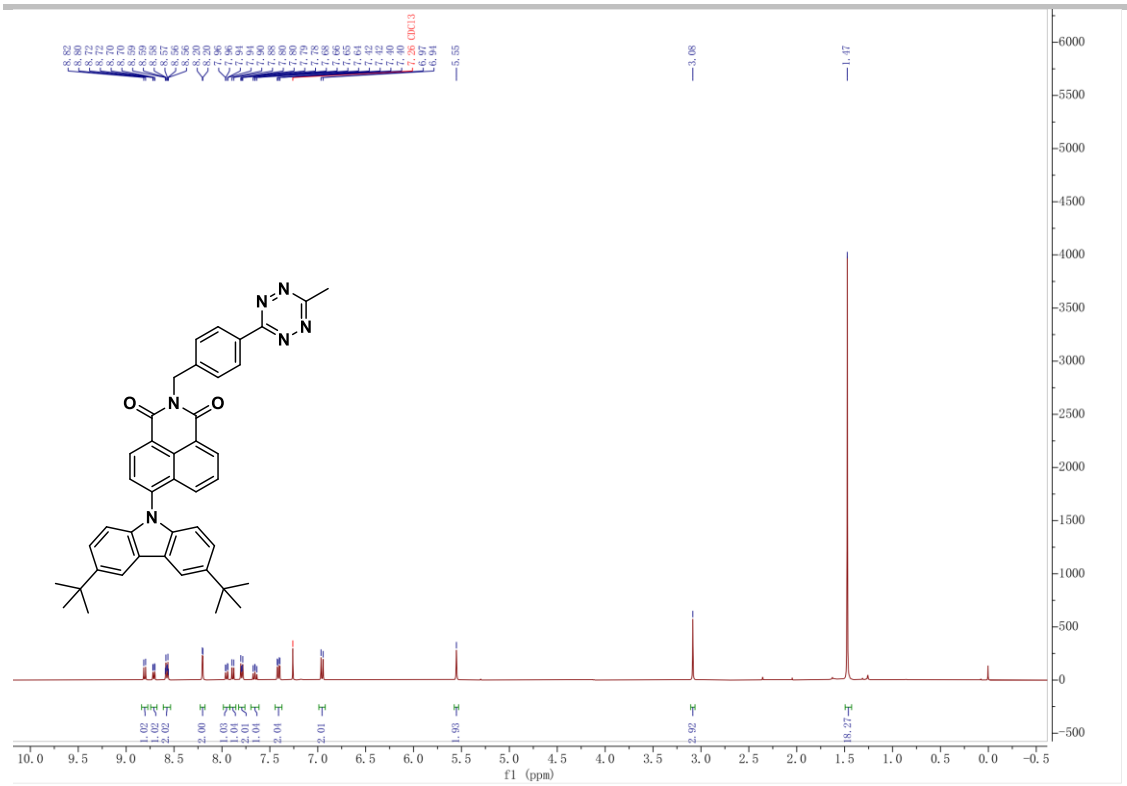

^{1}H NMR (400 MHz, Chloroform-*d*) of **Tz-NA**

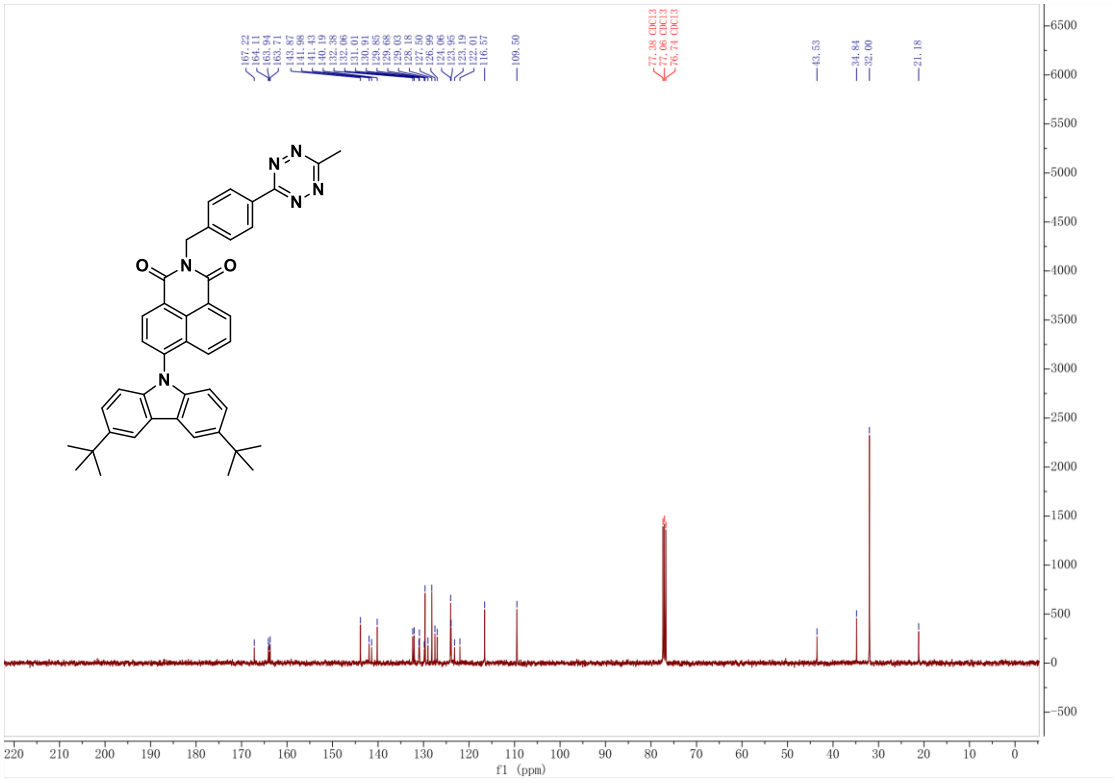

^{13}C NMR (101 MHz, Chloroform-*d*) of **Tz-NA**

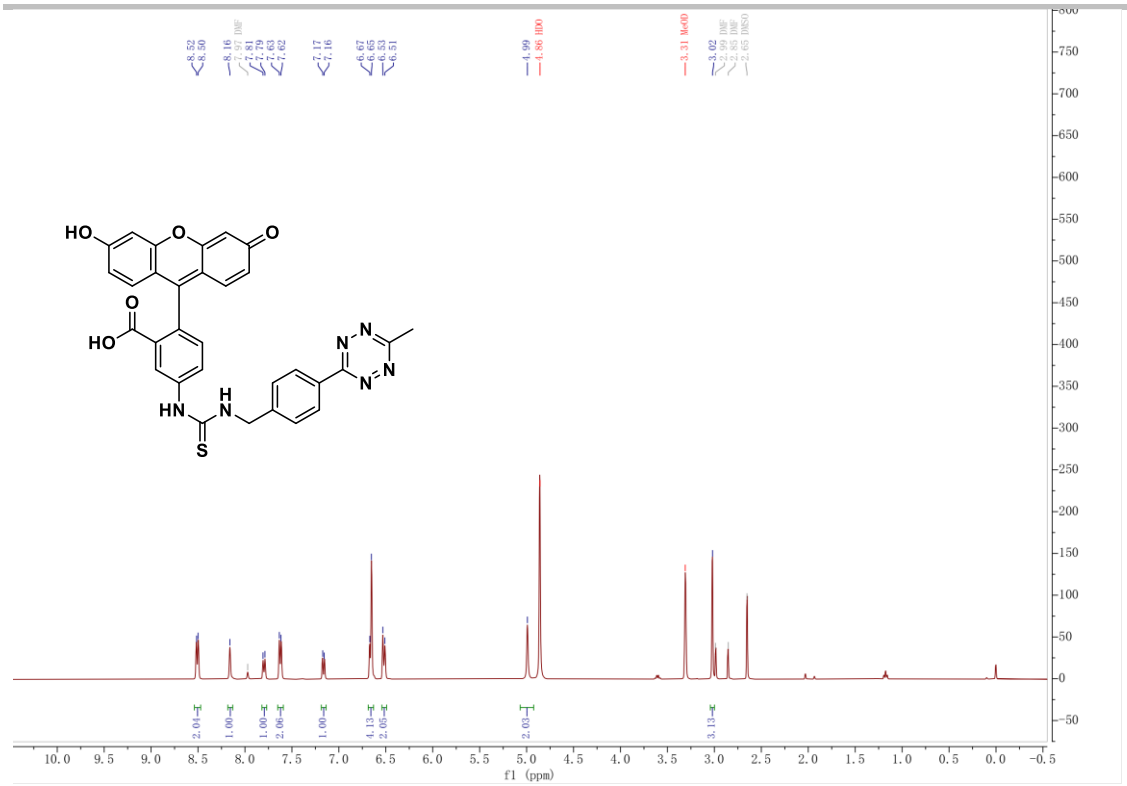

^{1}H NMR (400 MHz, Methanol-d_4) of **Tz-FL**

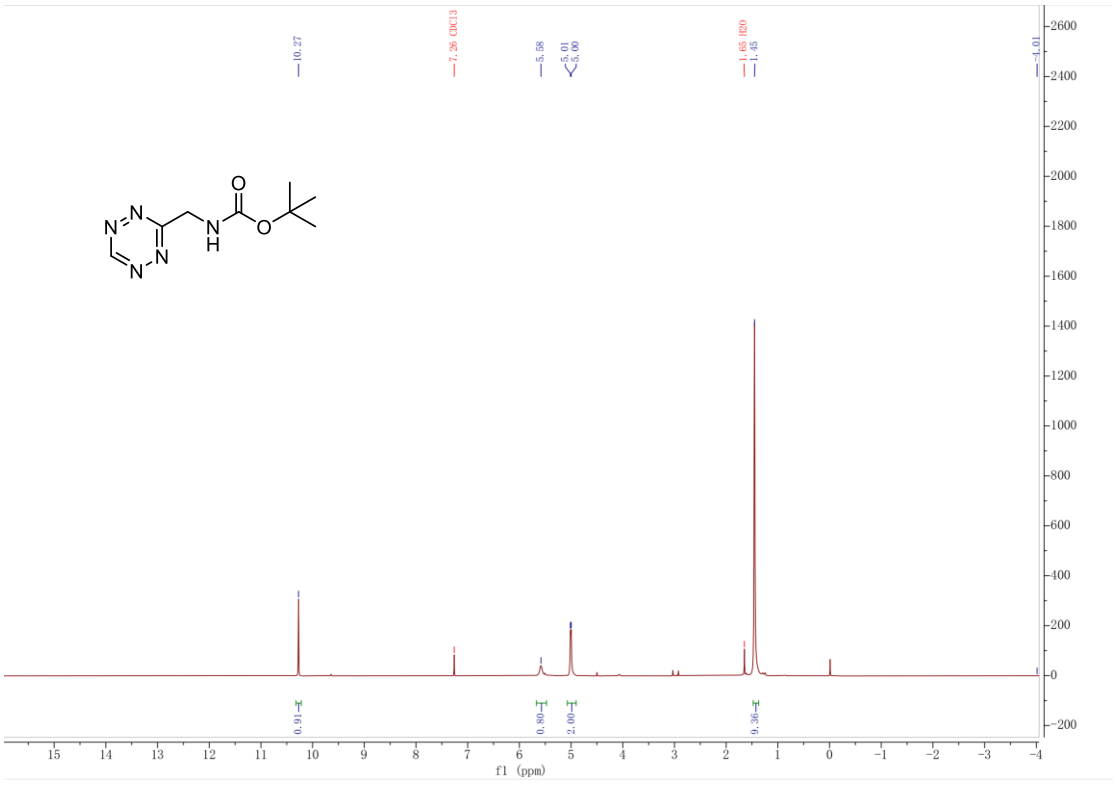

^{1}H NMR (400 MHz, Chloroform-*d*) of compound (14)

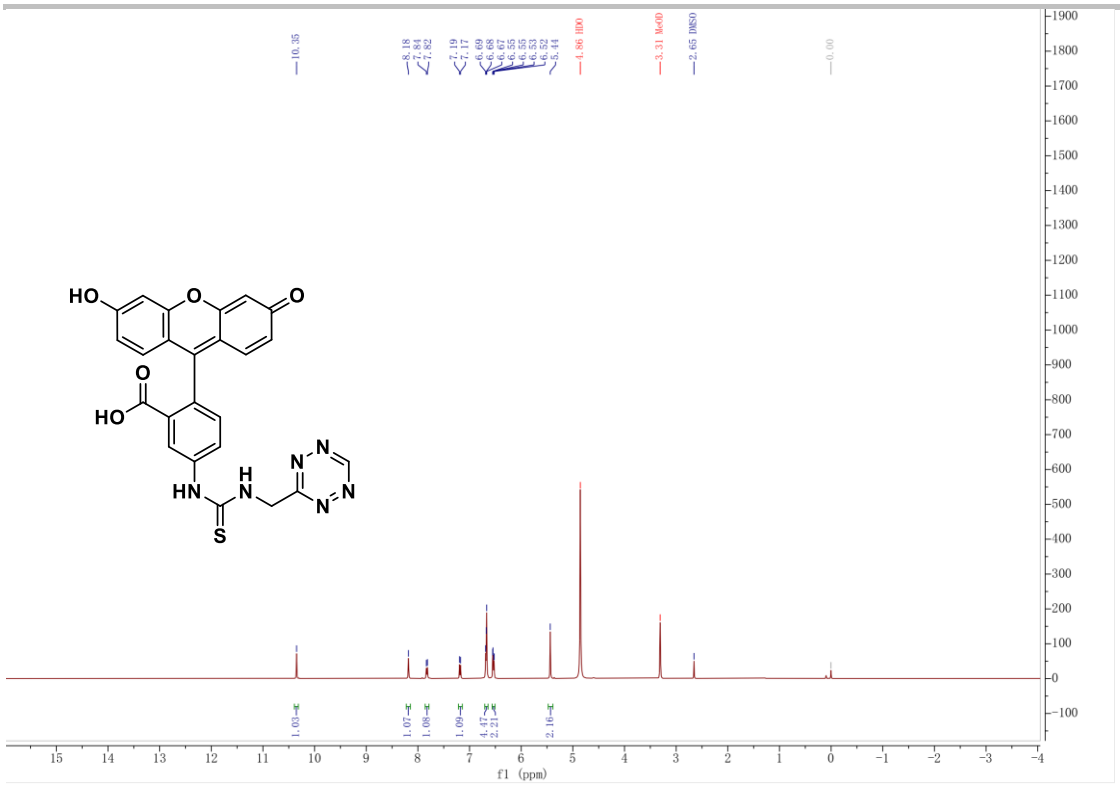

^{1}H NMR (400 MHz, Methanol-d_4) of **Tz-FL-S**

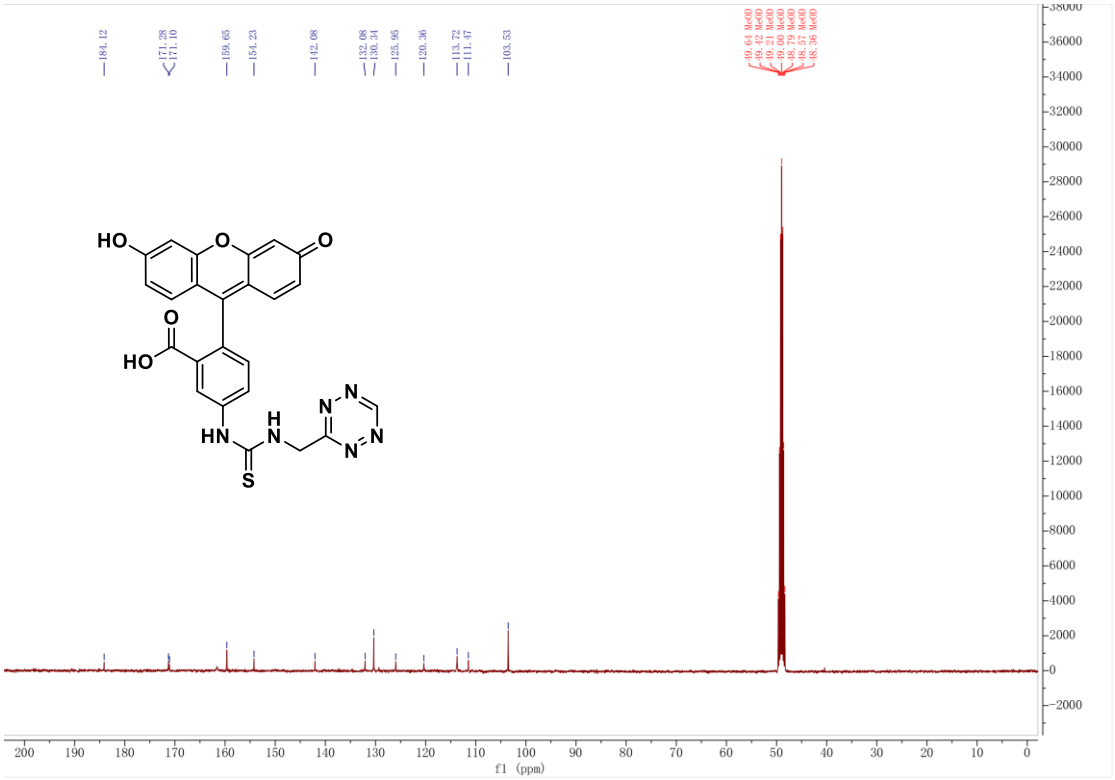

^{13}C NMR (101 MHz, Methanol-d_4) of **Tz-FL-S**

5. References

1. Wu, L.-L.; Wang, Q.; Wang, Y.; Zhang, N.; Zhang, Q.; Hu, H.-Y. Rapid Differentiation between Bacterial Infections and Cancer Using a Near-Infrared Fluorogenic Probe. *Chem. Sci.* **2020**, *11*, 3141–3145, doi:10.1039/D0SC00508H.
2. Siegl, S.J.; Vázquez, A.; Dzijak, R.; Dračínský, M.; Galeta, J.; Rampmaier, R.; Klepetářová, B.; Vrabel, M. Design and Synthesis of Aza-Bicyclononene Dienophiles for Rapid Fluorogenic Ligations. *Chemistry A European J* **2018**, *24*, 2426–2432, doi:10.1002/chem.201705188.
3. M. J. Frisch, G. W. Trucks, H. B. Schlegel, G. E. Scuseria, M. A. Robb, J. R. Cheeseman, G. Scalmani, V. Barone, G. A. Petersson, H. Nakatsuji, X. Li, M. Caricato, A. V. Marenich, J. Bloino, B. G. Janesko, R. Gomperts, B. Mennucci, H. P. Hratchian, J. V. Ortiz, A. F. Izmaylov, J. L. Sonnenberg, D. Williams-Young, F. Ding, F. Lipparini, F. Egidi, J. Goings, B. Peng, A. Petrone, T. Henderson, D. Ranasinghe, V. G. Zakrzewski, J. Gao, N. Rega, G. Zheng, W. Liang, M. Hada, M. Ehara, K. Toyota, R. Fukuda, J. Hasegawa, M. Ishida, T. Nakajima, Y. Honda, O. Kitao, H. Nakai, T. Vreven, K. Throssell, J. A. Montgomery, Jr., J. E. Peralta, F. Ogliaro, M. J. Bearpark, J. J. Heyd, E. N. Brothers, K. N. Kudin, V. N. Staroverov, T. A. Keith, R. Kobayashi, J. Normand, K. Raghavachari, A. P. Rendell, J. C. Burant, S. S. Iyengar, J. Tomasi, M. Cossi, J. M. Millam, M. Klene, C. Adamo, R. Cammi, J. W. Ochterski, R. L. Martin, K. Morokuma, O. Farkas, J. B. Foresman, and D. J. Fox, Gaussian 16, Gaussian, Inc., Wallingford CT, **2016**.
4. Becke, A.D. Density-functional Thermochemistry. III. The Role of Exact Exchange. *The Journal of Chemical Physics* **1993**, *98*, 5648–5652, doi:10.1063/1.464913.
5. Scalmani, G.; Frisch, M.J.; Mennucci, B.; Tomasi, J.; Cammi, R.; Barone, V. Geometries and Properties of Excited States in the Gas Phase and in Solution: Theory and Application of a Time-Dependent Density Functional Theory Polarizable Continuum Model. *The Journal of Chemical Physics* **2006**, *124*, 094107, doi:10.1063/1.2173258.
6. Adamo, C.; Barone, V. Toward Reliable Density Functional Methods without Adjustable Parameters: The PBE0 Model. *The Journal of Chemical Physics* **1999**, *110*, 6158–6170, doi:10.1063/1.478522.
7. Grimme, S.; Antony, J.; Ehrlich, S.; Krieg, H. A Consistent and Accurate Ab Initio Parametrization of Density Functional Dispersion Correction (DFT-D) for the 94 Elements H-Pu. *The Journal of Chemical Physics* **2010**, *132*, 154104, doi:10.1063/1.3382344.
8. Grimme, S.; Ehrlich, S.; Goerigk, L. Effect of the Damping Function in Dispersion Corrected Density Functional Theory. *Journal of Computational Chemistry* **2011**, *32*, 1456–1465, doi:10.1002/jcc.21759.
9. Grimme, S.; Hansen, A.; Brandenburg, J.G.; Bannwarth, C. Dispersion-Corrected Mean-Field Electronic Structure Methods. *Chem. Rev.* **2016**, *116*, 5105–5154, doi:10.1021/acs.chemrev.5b00533.
10. Hehre, W.J.; Ditchfield, R.; Pople, J.A. Self—Consistent Molecular Orbital Methods. XII. Further Extensions of Gaussian—Type Basis Sets for Use in Molecular Orbital Studies of Organic Molecules. *The Journal of Chemical Physics* **1972**, *56*, 2257–2261, doi:10.1063/1.1677527.
11. Yanai, T.; Tew, D.P.; Handy, N.C. A New Hybrid Exchange–Correlation Functional Using the Coulomb-Attenuating Method (CAM-B3LYP). *Chemical Physics Letters* **2004**, *393*, 51–57, doi:10.1016/j.cplett.2004.06.011.
12. Schäfer, A.; Horn, H.; Ahlrichs, R. Fully Optimized Contracted Gaussian Basis Sets for Atoms Li to Kr. *The Journal of Chemical Physics* **1992**, *97*, 2571–2577, doi:10.1063/1.463096.
13. Schäfer, A.; Huber, C.; Ahlrichs, R. Fully Optimized Contracted Gaussian Basis Sets of Triple Zeta Valence Quality for Atoms Li to Kr. *The Journal of Chemical Physics* **1994**, *100*, 5829–5835, doi:10.1063/1.467146.
14. Le Bahers, T.; Adamo, C.; Ciofini, I. A Qualitative Index of Spatial Extent in Charge-Transfer Excitations. *J. Chem. Theory Comput.* **2011**, *7*, 2498–2506, doi:10.1021/ct200308m.
15. Liu, Z.; Lu, T. Optical Properties of Novel Conjugated Nanohoops: Revealing the Effects of Topology and Size. *J. Phys. Chem. C* **2020**, *124*, 7353–7360, doi:10.1021/acs.jpcc.9b11170.
16. Lu, T.; Chen, F. Multiwfn: A Multifunctional Wavefunction Analyzer. *Journal of Computational Chemistry* **2012**, *33*, 580–592, doi:10.1002/jcc.22885.
17. Humphrey, W.; Dalke, A.; Schulten, K. VMD: Visual Molecular Dynamics. *Journal of Molecular Graphics* **1996**, *14*, 33–38, doi:10.1016/0263-7855(96)00018-5.
18. Bandyopadhyay, A.; Cambray, S.; Gao, J. Fast Diazaborine Formation of Semicarbazide Enables Facile Labeling of Bacterial Pathogens. *J. Am. Chem. Soc*. **2017**, *139*, 871–878, doi:10.1021/jacs.6b11115.